Molecular characterization of a pathogenic Ser111Thr mutation in the astrocytic water channel Aquaporin-4

Ammna Farooq

Master Thesis

In cell biology, physiology, and neuroscience

60 credits
Department of Biosciences
Faculty of Mathematics and Natural Sciences

UNIVERSITY OF OSLO

2021

2021

Molecular characterization of a pathogenic Ser111Thr mutation in the astrocytic water channel Aquaporin-4

http://www.duo.uio.no/

Trykk: Reprosentralen, Universitetet i Oslo

Acknowledgements

This master project was carried out at the Institute of Basic Medical Sciences at University of Oslo at the Laboratory for Molecular Neuroscience under Prof. Mahmood Amiry-Moghaddam's supervision.

First of all, I would like to express my gratitude to my supervisor Mahmood Amiry-Moghaddam for giving me the opportunity to work in his lab. His generous and extremely positive approach has been very encouraging. His knowledge and passion for neuroscience has been inspiring. I appreciate his valuable scientific advice given during my work in this project, which has been extremely useful. Further, I specially want to thank my co-supervisor, Nadia Skauli who has guided me throughout this project and spent several hours with me in the lab, teaching me western blot, RT-qPCR, and statically analysis. In addition, spending time in microscopy and deliberating images with me. Her optimistic personality and generosity have been extremely motivating during these two years. I really appreciate her valuable scientific advice, and time she has spent teaching me and helping me out when needed. I especially thank her for the guidance to write this thesis.

I want to thank the lab engineers. Shreyas Rao for teaching me immunohistochemistry and spending time in the microscopy with me. His energetic and fun personality has made the lab work cheerful and his willingness to help whenever needed. I would like to thank Mina Frey for preparing all the animal material used in this project and I have always appreciated her advice and support which have been extremely encouraging.

I also want to thank PhD student Negar Zohoorian for her great friendliness and always willing to help me out during emergencies, and *forskerlinje*-student Shervin Banitalebi for his positive and helpful approach.

It has been a great experience to work with all of them, and a memorable and educational time spent where I have had so much fun – even outside the lab!

Finally, I want to express my gratitude to my family who have always supported and cared for me during hectic periods and been there for me when needed. I also want to thank my friends for their support and kind words.

Abstract

Aquaporin-4 (AQP4) is the predominant brain water channel protein. It is mainly localized at the astrocytic end-feet abutting brain microvessels or pial surface, where it is believed to be involved in brain water and ion homeostasis. Mislocalization, combined with up- or downregulation of AQP4 expression is observed in many neuropathological conditions. Moreover, recent studies have indicated a pro-inflammatory role of AQP4 in certain disease models. However, little is known about the causal role of AQP4 in these conditions. A newly discovered pathogenic Ser111Thr mutation in the AQP4 gene in a Norwegian patient might shed light on the pathological significance of AQP4 in the brain. This patient has progressive neurological signs and symptoms including gait ataxia and moderate cognitive impairment indicating that cerebellum and cortical areas might be involved. This is the only human mutation found in AQP4 which is known to be pathogenic, and which does not affect the water permeability of the AQP4 channels. Here, we investigated a novel mouse model with the Ser111Thr mutation in the AQP4 gene to assess whether this mutation can explain the pathological phenotype observed in the patient. Specifically, we investigated the expression and distribution of AQP4, and the extent of inflammation judged by expression of astrocytic and microglial markers in cerebellum, hippocampus, and parietal cortex of the mutant mice compared with the wild type littermates. Our results show decreased protein expression of AQP4 and the microglial marker Iba1 in the cerebellum of the mutant mice compared with the wild type littermates. We also observed changes at the mRNA levels of certain inflammatory genes in the cerebellum of the mutant mice. Further investigation, including behavioral tests and more thorough and quantitative analysis are needed to establish whether the Ser111Thr mutation can explain the pathological phenotype observed in the patient.

Key words: AQP4; Ser111Thr mutation; astrocytes; microglia; inflammation

List of Abbreviations

AQP – Aquaporin

AQP4 – Aquaporin-4

AQP9 - Aquaporin-9

AQP1 - Aquaporin-1

CNS – central nervous system

OAP – Orthogonal arrays or assemblies of intramembranous particle

BBB – blood brain barrier

GFAP – Glial fibrillary protein

ECS – Extracellular space

CSF – cerebrospinal fluid

ISF – Interstitial fluid

Iba1- Ionized calcium-binding adapter molecule 1

PKA – protein kinase A

PKC – protein kinase C

AQP4KO – Aquaporin-4 knock-out

AQP4ex – Aquaporin-4ex

MTLE – mesial temporal lobe epilepsy

PD – Parkinson disease

AD – Alzheimer's disease

TPA – Tissue plasminogen activator

H7 – 1-(5-isoquinoline sulfonyl)-2-methylpiperazine

DAPC – dystrophin-associated protein complex

α-syntrophin – alpha syntrophin

TJs – tight junctions

Cx30 – Connexin-30

Cx43 – Connexin-43

IF - Immunofluorescence

DAPI – 4',6-diamidino-2-phenylindole

WB - Western blotting

SDS PAGE – Sodium dodecyl sulphate-polyacrylamide gel electrophoresis

BSA – Bovine Serum Albumin

LB - Loading buffer

PVDF – hydrophilic polyvinylidene fluoride

qPCR – quantitative polymerase chain reaction

cDNA – complementary DNA

Hc – Hippocampus

Cb – cerebellum

Pcx – parietal cortex

Table of Contents

1 Introduction

Transcellular water transport is an important process for all living organisms. To achieve a stable internal environment in the human body, an efficient water transport is required. Generally, the movement of water occurs across the lipid bilayer in the plasma membrane (Amiry-Moghaddam & Ottersen, 2003), but this system alone cannot regulate the water permeability and the osmotic pressure. The rapid transcellular water movement across the cell membrane is explained by transmembrane water channels, termed Aquaporins (AQPs). They were first discovered in 1992 by Peter Agre (Agre et al., 2002). Aquaporins are divided into two sub-types I) aquaporins only permeable to water, and II) aquaglyceroporins permeable to small molecules such as glycerol in addition to water (Nagelhus & Ottersen, 2013). In the recent years, they have brought attention due to their involvement in many pathophysiological processes.

1.1 Brain Aquaporins

AQPs are widely expressed throughout the human body to regulate the transcellular water flow (Day et al., 2014). Currently, thirteen different aquaporins are known to be expressed in the human body. Three of which have been described at the protein and mRNA levels in the brain; Aquaporin-1 (AQP1), which is expressed in choroid plexus nearby the brain cavities, Aquaporin-9 (AQP9) which is expressed in astrocytes and the neuropil, and Aquaporin-4 (AQP4), the predominant brain aquaporin (Badaut et al., 2014; Jung et al., 1994; Prydz et al., 2020), which is the main focus in this thesis.

1.2 Aquaproin-4: Expression, localization, and function

Aquaporin-4 (AQP4), with a molecular weight of ~37 kDa, is the predominant water channel found in the central nervous system (CNS). It is widely expressed at the end-feet of the astrocytes, which are the most abundant glial cells of the brain. Astrocytes form processes facing the blood interface, termed perivascular end-feet membranes (Mathiisen et al., 2010). Due to its abundant expression in perivascular astrocytes, AQP4 is considered a marker for astrocyte polarization (Jing Yang et al., 2011). Recent studies have highlighted their role and function regarding neurological- and neurodegenerative diseases (Eid et al., 2005; Prydz et al., 2020; Xu et al., 2015; Xue et al., 2019; Jing Yang et al., 2011).

1.2.1 Structure and function of AQP4 in CNS

AQP4 is expressed in several tissues of the human body including brain, spinal cord, heart, retina, inner ear, muscles, gastrointestinal tract, kidney, and lungs (Day et al., 2014). Structurally, six alpha-helices span trough the membrane and five loops in both the apical and basolateral surfaces of the water channel are presented (Fig 1). Loop B and E are hydrophobic regions involving amino acids proline, arginine and asparagine collectively called NPA-motif (Nagelhus & Ottersen, 2013). The hourglass shape of AQP4 is explained by the fact that loops B and E overlap each other to form a pore with the narrowest diameter at 2.8 Å, which is similar to the diameter of a water molecule. The pore consists of arginine residue that prevent H_3O^+ and cations entering the water channel and in addition the proton flow is prevented by positively charged dipoles, which is important for the ATP synthesis (Nagelhus & Ottersen, 2013; Tani et al., 2009). These properties of AQP4 makes it extremely selective for transport of water molecules, not allowing the passage of ions or other substances (Nagelhus & Ottersen, 2013). Electron crystallography shows that AQP4 are assembled as tetramers in the plasma membrane (Hiroaki et al., 2006). All aquaporins consist of four monomers that are assembled as tetramers in the membrane (Nesverova & Törnroth-Horsefield, 2019). The AQP4 tetramers form larger clusters, referred to as orthogonal arrays of particles (OAPs) (Crane et al., 2009).

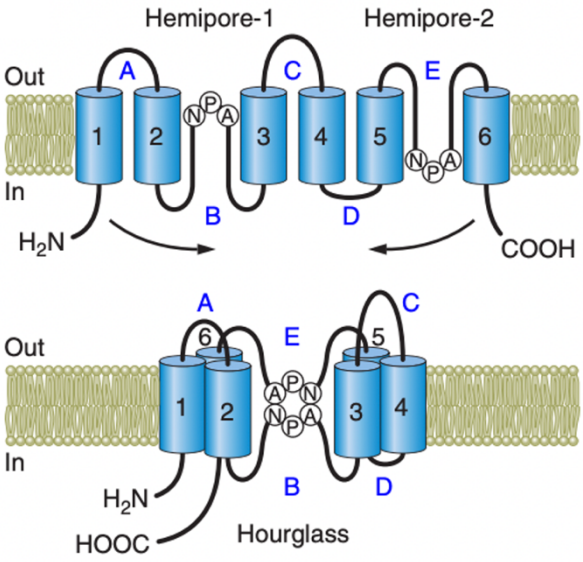

Figure 1: Diagram illustrating a single monomer of AQP4. The six helices (1-6) are spanning through the membrane and five loops (A-E) are presented both intra- and extracellularly. Loop B and E, consisting of NPA-motif, overlaps and form the pore which gives AQP4 the hourglass shape. Adapted from (Nagelhus & Ottersen, 2013).

A thorough analysis of the rat *Aqp4* gene, done by Moe et al 2008, shows six cDNA isoforms encoding for AQP4, referred to as *Aqp4a-f,* (Moe et al., 2008). Isoforms *Aqp4a* and *Aqp4c,* also referred to as M1 (32 kDa, 323 aa) and M23 (34 kDa, 301 aa) (Amiry-Moghaddam & Ottersen, 2003; Nagelhus & Ottersen, 2013), which are named after different translation initiation methionine sites (Neely et al., 1999). They are known as the classic isoforms and their expression, as heterodimers, determines the size of the AQP4 OAPs in the plasma membrane (Jung et al., 1994; Nicchia et al., 2008). The OAPs are largely composed by M23 isoform and due to this, M23 is the most important determinant of OAP size (Nicchia et al., 2008). Moreover, the water permeability appears to be the same in both isoforms (Nagelhus & Ottersen, 2013). Lately, an extended isoform encoding for AQP4 was discovered by Palazzo et al 2019, which is involved in anchoring of AQP4 at the astrocytic end-feet. The isoform is referred to as AQP4ex due to extension of AQP4 with 29-amino-acids at the C-terminal, and constitute approximately 10% of the AQP4 in the brain (Palazzo et al., 2019).

1.2.2 Expression and localization of AQP4 in the CNS

The areas that are abundant with AQP4 are referred to as primary sites of water flux which is mainly through astrocytic end-feet. Collectively, enriched expression of AQP4 at astrocytic end-feet abutting capillaries form important processes, termed perivascular end-feet (Nagelhus & Ottersen, 2013). AQP4 is also expressed at the astrocytic processes in the neuropil, the region with the neuronal compartments, where it is suggested to contribute to clearance of K^+-ions (Amiry-Moghaddam & Ottersen, 2003; Nielsen et al., 1997). Electrophysiological studies show increased seizure duration in AQP4-null animals, and increased extracellular K+ concentration, suggesting AQP4 is involved in regulation of K^+ ions (Binder et al., 2006; Vandebroek & Yasui, 2020).

In addition, AQP4 is enriched in the basolateral membrane of ependymal cells lining ventricle (Nielsen et al., 1997; Palazzo et al., 2019), which are cavities filled with cerebrospinal fluid (CSF) (Del Bigio, 2010). The CSF has protective role in the brain where it contributes to remove waste molecules to maintain the brain homeostasis (Telano & Baker, 2021). The abundant expression of AQP4 in the CSF- and brain-blood interface, allows it to participate in bidirectional water flux (Mahmood Amiry-Moghaddam et al., 2003; Mader & Brimberg, 2019; Nagelhus & Ottersen, 2013). This feature of AQP4 is suggested to be beneficial due to removal of excess water during vasogenic cerebral edema – a condition where water is accumulated in

the brain ECF (Verkman et al., 2006) and normophysiological water flux, for example recently shown during sleep (Bojarskaite et al., 2020).

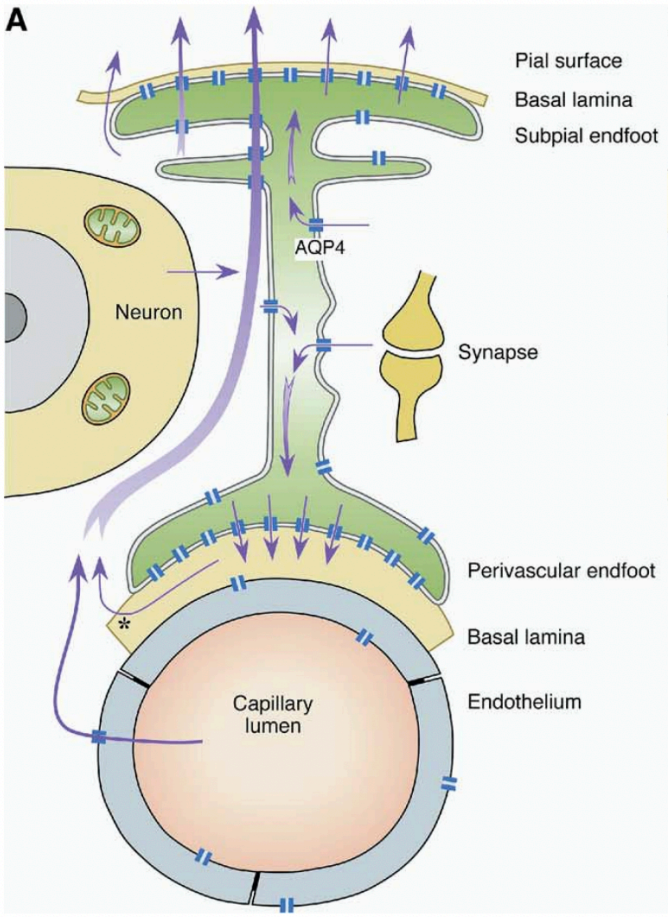

Figure 2: Illustration of enriched AQP4 (blue) expression at astrocytic end-feet and subpial membranes. AQP4 in astrocytes are expressed in high density at the blood interface, forming perivascular astrocytic processes. Hypothetically, the arrows show water flow in the brain which is mediated by AQP4. Adapted from (Amiry-Moghaddam et al., 2004).

1.3 Physiological roles of AQP4

The physiological role of AQP4 is not well known, but likely contributes to important processes such as regulation of extra cellular space (ECS) volume in the brain. During synaptic activation, accumulation of solutes including glutamate, K^+, and bicarbonate occurs in the ECS which are suggested to co-transport with water through perisynaptic end-feet. ECF volumes are altered during excitatory synaptic activation, in hippocampus of AQP4 deficient animals, compared to wild type mice (Haj-Yasein et al., 2012). This evidence suggests that ECS shrinkage is normally

prevented by AQP4 which facilitates water efflux through perisynaptic end-feet during high synaptic activation.

In addition, AQP4 facilitate the waste clearance system of CNS, which is referred to as glymphatic system that resembles the lymphatic clearance system. Importantly, there are two types of fluid in the brain; the interstitial fluid (ISF) surrounding the brain parenchyma in the interstitial space, and the CSF, produced by choroid plexus and distributed in the brain through ventricles (Lun et al., 2015). CSF has a protective role by removing waste and toxins (Silva et al., 2021). The brain fluids are important components of the glymphatic system and prevent misaccumulation of waste products in the brain (Nedergaard, 2013). Any disturbance in this system is pathogenic. Apparently, it shows that AQP4 contributes in the in regulation of the glymphatic system (Silva et al., 2021) by promoting the CSF flux in the brain. To begin with, the CSF influx is in the brain mediated through pial vessels that transport fluid down to perivascular space, which is region between astrocytic end-feet and blood vessel. AQP4s are highly expressed at the blood interface at astrocytic end feet where it promotes a convective CSF flux into the intestinal space, where it mixes with the ISF (Nedergaard, 2013). Moreover, CSF-ISF allows the clearance of waste products, by leaving the brain through perivenous efflux and into the systemic circulation (Nedergaard, 2013; Silva et al., 2021). AQP4 deficient animals shows that trace influx of CSF is reduced compared to WT-AQP4 (Mestre et al., 2018). This evidence strongly provides important knowledge about the role of AQP4 in the brain clearance system.

1.4 Pathophysiology involving AQP4

1.4.1 Brain edema: cytotoxic and vasogenic

Accumulation of water in the brain can consequently cause disruption of the brain homeostasis, resulting in a pathogenic condition. AQP4 has been shown to play an important role in the development of brain edema (Amiry-Moghaddam et al., 2004; Ma et al., 1997), which is brain swelling due to accumulation of fluid in the ECS (Nehring et al., 2021). The accumulation of water in the brain is referred as either 1) vasogenic cerebral edema and 2) cytotoxic cerebral edema. Vasogenic cerebral edema is caused by increased BBB permeability which allows the plasma fluid – including water and other substances entering brain (Koenig, 2018), and promoting brain swelling. In contrast, accumulation water within the brain cells without

disruption of the BBB i.e., mainly caused by astrocytic swelling, is referred as cytotoxic cerebral edema (Verkman et al., 2006). Both edema types are involved in neuropathologies such as stroke.

AQP4 deficient animals have been useful to study the role of AQP4 during cerebral edema. Two important disease models of cerebral edema – 1) ischemic stroke and 2) acute water intoxication, have provided insight into the importance of the pathogenic role of AQP4 during development of brain edema (Manley et al., 2000; Verkman et al., 2006). A study done by Manley et al 2000, shows survival and reduced cerebral edema in AQP4-null mice subjected with ischemic stroke and acute water intoxication (Manley et al., 2000). In contrast, upregulation of AQP4 has shown a beneficial role – due to removal of excess water during development of vasogenic cerebral edema (Chi et al., 2011; Verkman et al., 2006). These studies indicate that the role and function of AQP4 is both beneficial and harmful depending on the disease model.

Cerebral edema is associated with neurological diseases including ischemic stroke and brain tumors (Manley et al., 2000). Surprisingly, the expression of AQP4 during disease has been stated to be both harmful and protective, suggesting a complicated regulation. The regulatory mechanism governing AQP4 expression and localization is currently unknown.

1.4.2 Neurological and neurodegenerative diseases related to AQP4

One important feature of AQP4 which is observed during pathological conditions is mislocalization of this water channel in perivascular end-feet membranes. This feature is a common denominator found in diseases including Alzheimer's disease, temporal lobe epilepsy, and Parkinson disease. We will briefly discuss the role of AQP4 in these disease conditions.

Epilepsy

Epilepsy is neurological disorder that disturbs the brain activity causing seizures in the patient. As earlier reported, astrocytes contribute to regulate the K^+ ions in the ESC, which is extremely important for neuronal homeostasis. Previous studies have shown that mislocalization of AQP4 has caused delay in K^+ and enhances epileptic seizures in mice (M. Amiry-Moghaddam et al., 2003).

Mesial temporal lobe epilepsy (MTLE) is caused by accumulation of K^+- ions in the ECS which make the neurons highly excitable. The disease triggers seizures from mesial temporal lobe including mainly hippocampus, termed MTLE hippocampus (Eid et al., 2005). During MTLE, hippocampus undergoes changes and becomes more hardened, a process termed sclerosis (Dudek & Rogawski, 2005). A study by Eid et al 2005, shows that AQP4 expression at protein level in MTLE hippocampus is upregulated. Investigation of localization of AQP4 resulted loss of AQP4 polarity in the perivascular end-feet in CA1 region of MTLE hippocampus compared to non-MTLE hippocampus. Furthermore, the expression of dystrophin which is an important component in anchoring AQP4 leading to its polarized expression was investigated. Reduction in DP71, a major isoform of dystrophin, was observed in CA1 region of MTLE hippocampus (Eid et al., 2005). Mislocalization of AQP4 from the perivascular end-feet in CA1 region is suggested to cause alteration in water permeability and disturbance in regulation of K^+- ions mediated by astrocytes, which eventually enhances epileptogenesis in the brain (Dudek & Rogawski, 2005).

Alzheimer's disease

Alzheimer's disease (AD) is a type of dementia leading to cognitive and memory dysfunction. The disease is characterized by brain atrophy likely due to upregulation of a protein called amyloid beta. Accumulation of this protein in CNS contribute to neuronal death by forming plaques in the synaptic cleft causing lack of communication between the neurons, which eventually lead to neuronal death. A study done by Yang et al 2011 shows that plaques formed by amyloid beta deposits at the perivascular end-feet lead to loss of astrocytic polarity – mislocalization of AQP4 (J. Yang et al., 2011). This study might provide important insight into the involvement of AQP4 during development of AD, since it clearly shows that the loss of astrocytic polarity is found at the perivascular end-feet, while AQP4 expression at the neuropil plaques is upregulated (J. Yang et al., 2011).

Parkinson disease

Parkinson disease (PD) is a neurological disorder which affects the motor system in the CNS The disease mainly affects the basal ganglia and substantia nigra regions of the brain (Blandini et al., 2000). Most cases are idiopathic and are characterized by extensive loss of dopamine-producing neurons in the substantia nigra together with slowness of movement, tremor, and bradykinesia (Zhang et al., 2020). A recent study done by Prydz et al 2020, shows abundant

expression of AQP4 on protein- and mRNA levels in the substantia nigra during development of PD. To create a PD model and study the role of AQP4 in PD, both wild type and AQP4 knockout animals were injected with a parkisonogenic toxin leading to selective loss of dopaminergic neurons in the substantia nigra, simulating the human disease process. Here, it was found that AQP4 played a pro-inflammatory role and enhanced the severity of PD (Prydz et al., 2020). Normally, during pathological neuroinflammatory processes reactive astrocytes are induced by microglia activation (Liddelow et al., 2017). Prydz et al 2020, shows that the genes which are normally highly expressed during microglia activation including *Trem2, Cd14, Cxcr1* and *Itgam* were not upregulated in AQP4KO animals treated with MPP+ (Prydz et al., 2020). Additionally, the decreased inflammatory response in AQP4-null mice has been shown to be related to the downregulation of expression of important immunosuppressive regulators which exacerbates PD pathogenesis in mice (Chi et al., 2011). This evidence suggests that both microglial activity is strongly affected by the disturbed communication between astrocytes and microglia in AQP4KO animals.

1.4.3 Regulation of AQP4 expression in the brain

AQP4 expression, and its polarized distribution is altered in several neurological and neurodegenerative disorders (Eid et al., 2005; Frydenlund et al., 2006; Jing Yang et al., 2011) It is important to understand how AQP4 expression and polarization in astrocytes is regulated, and several studies has tried to clarify this question.

Protein Kinase C (PKC) is a kinase triggering a major transduction cascade that regulates various intracellular responses including growth, expression, and localization of various proteins. Normally, protein kinases are involved in regulation of various proteins by phosphorylating the hydroxyl group of serine and threonine residues (Sun & Alkon, 2012). Serine/threonine kinases are abundantly found in the CNS, and neurodegenerative diseases such as ischemia and AD have shown dysregulation of the serine/threonine kinases mediated by PKC activation (Domańska-Janik, 1996; Sun & Alkon, 2012). Previous studies (Nakahama et al., 1999; Yamamoto et al., 2001) suggest that protein kinase C (PKC) is involved in the regulation of AQP4 expression (Amiry-Moghaddam & Ottersen, 2003) through an unknown mechanism.

Regulation of AQP4 expression mediated by PKC is an interesting topic that remains unclear. Nakahama et al 1999 was the first study to show that tissue plasminogen activator (TPA) treated astrocytes result a significant decrease in the mRNA levels of AQP4 that is mediated by PKC activation. The astrocytes were pretreated with a PKC inhibitor, 1-(5-isoquinoline sulfonyl)-2-methylpiperazine (H7). A control group, with untreated astrocytes, was also included. Surprisingly, the TPA cells, with H7 treated astrocytes showed a significant decrease in AQP4 mRNA levels (Nakahama et al., 1999). This study provides an insight into how PKC activation play a role in the regulation of AQP4 expression in astrocytes.

Considering the absence of inhibitors and regulatory mechanisms for AQP4, mutations are the most important tool for investigation of the role and function of the water channel. Important amino acid residues in AQP4 have been studied to determine the regulatory mechanism of the water channel. Phosphorylation of the Serine111 residue, found in the cytoplasmic loop B of AQP4 (Nesverova & Törnroth-Horsefield, 2019), has not shown significant changes in the water permeability of AQP4 (Assentoft et al., 2013). Notably, this serine is a highly conserved residue found in almost all aquaporins (Berland et al., 2018).

Mutations of the Ser111 residue in AQP4 indicates to be important for stability and function of AQP4 in in vitro experiments. A study by Silberstein et al 2004 shows that when the S111 residue is mutated with glutamic acid (S111E) there is observed upregulation of OAPs formed by M23-AQP4 isoform. Hypothetically, this have led researchers to speculate that Ser111 could potentially be a phosphorylation site targeted by PKA (Silberstein et al., 2004).

Previous studies strongly suggest that phosphorylation of Ser111 contribute to regulation of glutamate and potassium in the brain. Both studies; Gunnarson et al 2008 and Song & Gunnarson, 2012, shows that substitution of Ser111 to alanine (Ser111Ala) has an impact on the levels of glutamate and potassium (Gunnarson et al., 2008; Song & Gunnarson, 2012). The true function of serine residues in AQP4 still remains a debated topic. Increase of extracellular potassium correspond to increase astrocytic water permeability. Phosphorylation of Ser111 in AQP4, showed a significant increase of potassium concentration in ECS while Ser111A did not show any significant changes (Song & Gunnarson, 2012).

Interestingly, AQP4 is not the only protein that mediates water flux in the brain. Another class of proteins called connexins form gap junctions between cells in the CNS. In astrocytes, connexin-43, and Connexin-30 (Cx30) are expressed. The gap junctions generated by these

connexins connect astrocytic cytoplasm to form networks mediating water and ion flux. In AQP4-KO animals, Cx43 and Cx30 have been shown to be upregulated to compensate for the loss of AQP4 (Katoozi et al., 2017).

1.4.4 Regulation of AQP4 localization in the brain

The expression of AQP4 in the perivascular end-feet membranes is crucial for maintaining the brain homeostasis. As reported, the water channel contributes to formation of an extremely selective BBB, which prevent dangerous substances from entering the brain. Any disturbance in this system can be pathogenic. Loss of astrocytic polarity i.e., mislocalization of AQP4 is often found in several neurological- and neurodegenerative diseases including Alzheimer disease, stroke, and epilepsy (Eid et al., 2005; Frydenlund et al., 2006; Jing Yang et al., 2011). The involvement of dystrophin-associated protein complex (DAPC) shows to be an important determinant for localization of AQP4 in the perivascular end-feet membranes (Mahmood Amiry-Moghaddam et al., 2003; John D. Neely et al., 2001). These studies along with other showed that anchoring of AQP4, in the end-feet membranes, is mediated by α-syntrophin and dystrophin (J. D. Neely et al., 2001). In absence of α-syntrophin, judged by immunohistochemistry and immunogold labeling of AQP4, reveals loss of astrocyte polarity which signifies mislocalization of the water channel from perivascular membranes (Amiry-Moghaddam et al., 2004).

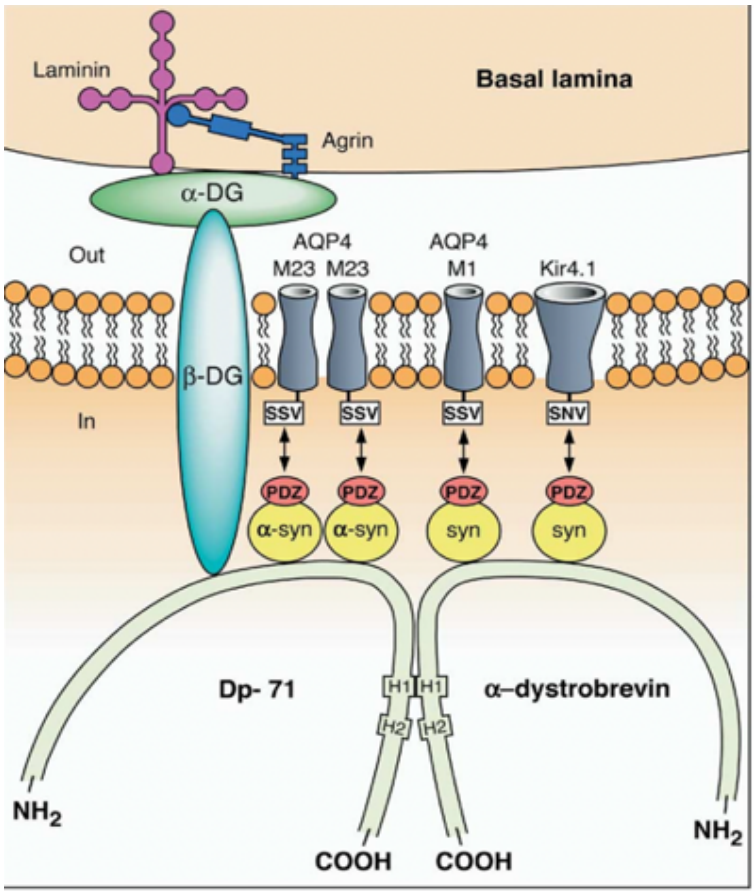

Figure 3: Schematic illustration of AQP4 anchoring at perivascular end-feet. An indirect linkage between α-syntrophin and AQP4 (M23) through PDZ binding domains is illustrated, while other syntrophins are anchoring M1 isoform. The major isoform of α-syntriohin is represented as Dp-71 and linked to α-dsytrobervin through motif interaction, termed H1. Dystrophin complex binds to AQP4 by being anchored to basal lamina by Laminin and Agrin. Adapted from (Amiry-Moghaddam et al., 2004).

A novel isoform of AQP4 termed AQP4ex was recently discovered by Palazzo et al. 2019. This isoform is involved in the proper membrane localization of AQP4 in the mouse brain. The study shows an assessment of the effect AQP4ex has on the perivascular end-feet in blood interface. By generating AQP4ex-KO mice, several functions of AQP4 were observed including the main function – the water transport, expression, and localization of the water channel. There was not observed significant changes in the water permeability of AQP4 in AQP4ex-KO mice (Palazzo et al., 2019). Interestingly, two important discoveries were provided to give an insight into the function of the large OAPs. To begin with, a significant change in the size of AQP4-OAPs was shown in AQP4ex deficient mice. Smaller size of OAPs was observed, while the number was unaltered. Most importantly, AQP4ex-KO mice resulted mislocalization of AQP4 from the perivascular end-feet membranes. The expression of dystrophin was unaltered, while a

significant decrease was observed in the expression of α-syntrophin (Palazzo et al., 2019). These findings suggest that AQP4ex, together with α-syntrophin, is an important determinant for the localization of AQP4 in the brain.

1.5 Non-channel functions of AQP4

The function and role of AQP4 has been investigated in the neurological- and neurodegenerative diseases mentioned above. It has become clear that AQP4 has several functions not related to water permeability. For example, they are involved in regulating neuroinflammation in addition to water transport (Chi et al., 2011; Prydz et al., 2020). In pathological conditions, the brain undergoes neuroinflammatory processes which is important hallmark for many neurological and neurodegenerative diseases. In a mouse model of intratarsal injection of parkinsonian toxin, AQP4-null showed significantly less inflammation and microglial activation compared to the WT (Prydz et al., 2020). AQP4-null mice have been beneficial to study e.g., astrocytes and microglia which shows an interaction with AQP4.

Since AQP4 is mainly expressed in astrocytes, knowledge about their function may shed light on possible mechanisms by which AQP4 can become pathogenic. Furthermore, we will discuss the physiological and pathophysiological role of astrocytes which are the abundant glial cells of the brain, additionally look at the role of microglia, the immune cells of the brain.

1.6 Astrocytes – the housekeepers of the brain

Astrocytes were named after their star-shaped appearance by Michael von Lenhossek in 1891 (Parpura & Verkhratsky, 2012). As previously mentioned, they contribute to many functions, including regulation of the extracellular fluid composition and waste removal (Haj-Yasein et al., 2012; Mestre et al., 2018). Astrocytes are classified according to their morphology which vary per type. The most common structure of the astrocytes consists of a cell body (soma), from which many branches are extended. These branches are often called «processes» or «astrocytic endfeet». The extensions of these branches endow the astrocytes with perisynapitc processes. The endfeet of astrocytes surrounding the brain capillaries are known as perivascular endfeet. Astrocytic processes can extend to the brain surface, abutting pia mater ; such processes are referred to as subpial end-feet (Mathiisen et al., 2010).

Astrocytes are widely represented in the CNS and constitute approximately 80% of the glial cells. During the last 20 years, research on astrocytes has received more attention due to the roles and functions of these cells in health and disease. The classical star shaped morphology of astrocytes relies on the expression of its intermediate filament proteins which are crucial in formation of the cytoskeleton. The Glial Fibrillary Acidic Protein (GFAP) and vimentin are the intermediate filament proteins highly expressed in astrocytes (Wilhelmsson et al., 2019). GFAP in particular is a specific marker for astrocytes and is not expressed in other cell types in the adult brain.

1.6.1 The many functions of astrocytes in CNS

In many ways, astrocytes act as supportive cells of the neurons, that are extremely excitable cells needing to be protected in a stable environment (Banerjee & Bhat, 2007). The microenvironment in the CNS is maintained by astrocytes, where they mainly contribute to balance the concentration of ions (i.e., K^+) and neurotransmitters (i.e., glutamate and GABA). In addition, astrocyte are involved in the repair of brain injury and modulation of synapses (Kim et al., 2019) which will be further discussed.

The neuronal excitability depends on formation of the K^+-gradient, where the concentration of K^+ is low in the extracellular space and higher inside the neurons. To prevent excessive K^+ in the extracellular space, the astrocytes act as a spatial buffer by taking up K^+ ions through inward rectifying potassium channels, termed Kir.4.1 channels (Kim et al., 2019). In addition, astrocytes also regulate homeostasis of important neurotransmitters, such as glutamate which is an major excitatory transmitter (Zhou & Danbolt, 2014). Accumulation of glutamate in the extracellular space (ECS) leads to a process called «excitotoxicity» which eventually cause death of nerve cells (Zhou & Danbolt, 2014). Excitotoxicity, caused by excessive glutamate in the ECS, is associated with neurodegenerative disease e.g., Alzheimer's disease (AD) ischemia, epilepsy, and Parkinson disease (PD) (Pajarillo et al., 2019). Astrocytes ensure that the excessive glutamate, assembled in synaptic cleft, is recycled back to the neurons (Kim et al., 2019). Furthermore, glutamate is recycled back to neurons in form of glutamine, and thereby converted to glutamate inside the neurons by an enzyme called glutamine synthase (Underhill & Amara, 2009). Additionally, astrocytes along with microglia also contribute to synapse remodeling during brain development where they act as highly phagocytic astrocytes (Chung et al., 2013).

Besides being supportive cells of the neurons, astrocytes are involved in forming an important structure in the brain which is a highly selective barrier between the capillary system and the brain, referred to as blood-brain barrier (BBB). The formation of the BBB requires astrocytic end-feet, a basal lamina composed of endothelial cells, extracellular matrix, and pericytes (Abbott et al., 2006), which are contractile cells of the capillaries and embedded in the walls of the vessels (Attwell et al., 2016).

The selectivity for the transport of substances within the brain is regulated by important structure formed by the endothelial cells known as tight junctions (TJs). These play an important role in formation of BBB by decreasing its permeability (Haseloff et al., 2015). Diffusible molecules including O_2, CO_2 and lipid soluble substances pass through the plasma membrane meanwhile transport of other substances e.g., ions (i.e., Na^+, Cl^-), amino acids and glucose need specialized transmembrane proteins to pass the barrier (Fong, 2015).

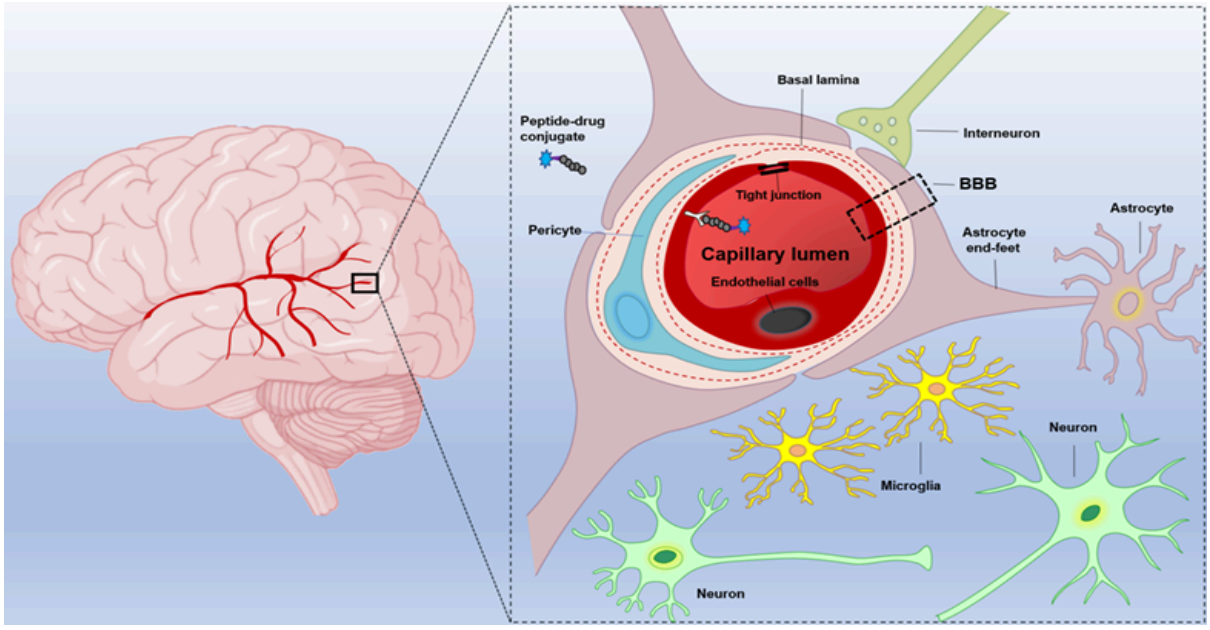

Figure 4: Diagram illustrating components of the blood-brain barrier. The endothelial cells form the BBB with perivascular end-feet that surround the blood vessel. Tight junctions are presented between the endothelial cells by limiting supply of substances to brain. Adapted from (Zhou et al., 2021)

1.7 The role of astrocytes in pathophysiology

Neuropathology is a term describing disease processes in the nervous system, such as neurodegeneration and brain injury. Astrocytes along with microglia are responsible for generating neuroinflammatory environments in the CNS. In response to an insult or injury, both pro- and anti-inflammatory phenotypes are induced (Liddelow & Barres, 2017). Interestingly, astrocytes undergo changes in their morphology, expression, and function as a response to pathogenesis or brain injury. The transformation of the expression and morphology in astrocytes , is referred to as «astrogliosis» and transformed astrocytes are referred to as «reactive astrocytes» (Liddelow et al., 2017). Reactive astrocytes are among others, identified by their upregulation of GFAP, which is often studied by immunolabeling of GFAP. GFAP labeling shows during pathogenies astrocytes undergo an alteration where they result in «aggressive» phenotype by receiving remarkable transformation in their morphology and expression pattern (Liddelow & Barres, 2017). GFAP expression is upregulated both on protein- and mRNA levels during various pathological conditions e.g., late stages in Alzheimer's disease (Middeldorp & Hol, 2011; Zhou et al., 2019). These features of GFAP makes it an important hallmark protein in reactive astrocytes and during neuroinflammation.

In the healthy brain astrocytes are main contributors of creating homeostasis for neuronal activity. However, it has been suggested that reactive astrocytes can play a neurotoxic role during pathogenesis, inhibiting the function of neurons and leading to neuronal death. The true function of reactive astrocytes is debatable. Previous studies suggest that there are, at least, two main types of reactive astrocytes, termed A1 and type A2 (Liddelow & Barres, 2017). Type A1 is considered to induce inflammatory environment and has a neurotoxic role by releasing neurotoxic factors during disease. The A1 phenotype is primarily induced by cytokines (IL-1a, TNFα and C1q*)* produced and secreted by microglia. Type A2 has been suggested to be a «non-harmful» phenotype which secretes neurotrophic factors to promote neuronal homeostasis (Liddelow & Barres, 2017).

Some important features of astrocytes appear to be absent in the A1 types, including their highly phagocytic function and their support to neuronal growth (Liddelow & Barres, 2017). Liddelow et al 2017 show that type A1 astrocytes are highly involved in neurodegenerative diseases including Alzheimer's disease (AD), Parkinson disease (AD) and multiple sclerosis (MS). One analysis of tissues from patient with AD showed that 60% of astrocytes constituted of type A (Liddelow et al., 2017). Currently, the mechanisms involved in neuronal death mediated by

astrocytes during pathological conditions is being widely investigated and is not completely understood.

1.8 Microglia

Microglia are small cells often considered the innate immune cells of the CNS, now known to originate from the hematopoietic stem cells (Nayak et al., 2014). Structurally, they resemble astrocytes but are smaller in size and consist of several shorter processes. Microglial activity depends on production of pro-inflammatory cytokines to prevent further brain damage but can also have detrimental effect in the brain (Smith et al., 2012). Similarly, to astrocytes, the microglia are expressed as subtypes, termed M1 and M2. The M1 type has protective role during pathological conditions by inducing anti-inflammatory response whereas while M2 microglia induces pro-inflammatory factors and exuberates pathogenesis (Tang & Le, 2016).

So far there is no completely specific method available to differentiate the heterogenous microglia (Salter & Stevens, 2017). However, certain genes are known as «risk genes» e.g., *Cx3cr1* which is a gene coding for chemokine receptors. During AD, deficiency of *Cxc3r1* induce detrimental conditions (Wolf et al., 2013). Investigation of this gene expression can be used to determine if the microglial activity is beneficial or detrimental during pathogenesis.

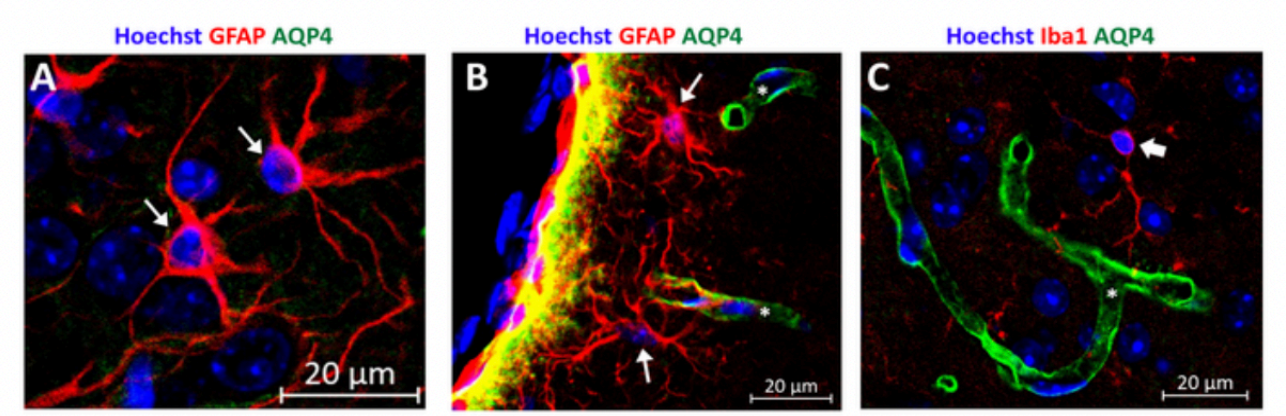

Figure 5: Immunolocalization of AQP4 GFAP and Iba1 in the brain. ***A)*** *Shows the star-like shape of GFAP-labeled astrocytes (red) which are abundantly expressed in the brain. The arrows indicate nucleus (blue) of astrocytes and neurons which are stained with Hoechst.* ***B)*** *The abundant expression of AQ4 (green) and GFAP (red) abutting the capillaries shows astrocytic end-feet along with AQP4 forming perivascular processes.* ***C)*** *Shows the immunolocalization of Iba1-labeled microglia (red) nearby capillaries, which are surrounded by AQP4 (green). Normally, astrocytes and microglia are co-localized and facilitate communication with each other. Confocal microscope images. Scale bar = 20 µm.*

1.9 A novel human disorder due to a Ser111Thr mutation in AQP4

Recently, a novel genetic disease was discovered in a Norwegian patient where the disease-causing mutation was found to be a heterozygous de novo mutation in AQP4 at the Ser111 residue. Here, the highly conserved Ser111 residue is changed to Thr on one allele (Berland et al., 2018). The patient exhibits several progressive disabilities including intellectual disabilities, transient signs of cerebral brain ischemia, transient cardiac hypertrophy, hearing loss and progressive gait disturbance (Berland et al., 2018). The presentation of this patients suggests that AQP4 is involved in the phenotype, especially brain ischemia detected after birth and progressive gait disturbance. Interestingly, some visual disturbance and hearing loss was also observed. AQP4 is highly expressed in retina (Amann et al., 2016) and AQP4KO mice exhibit hearing loss (Li & Verkman, 2001). The patient exhibits mild intellectual disability, which has also been shown in some strains of AQP4KO mice (Woo et al., 2018). Interestingly, this is the first case of a deleterious AQP4 mutation leading to a clear disease phenotype.

In the original study by Berland et al. 2018, it is shown that Ser111Thr does not affect the water permeability of AQP4. The wild type and Ser111Thr mutated AQP4 were introduced in *Xenopus laevis* oocytes, to compare the water permeability. There was not observed significant changes in the water permeability between wild type- and Ser111Thr AQP4 (Berland et al., 2018). As reported earlier, phosphorylation of serine residue in AQP4 mediated by PKC or PKA is suggested to be involved in regulation of AQP4 expression. Berland et al 2018 suggest that Ser111 might be a phosphorylation site that is targeted by PKA and involved in regulation of AQP4 expression and function (Berland et al., 2018).

1.10 Aims of the thesis

The objective of this project is to characterize mice with a pathogenic Ser111Thr mutation in the *Aqp4* gene, described in a patient with a wide range of symptoms from the CNS. The aim is to see whether the mutation leads to pathological changes, mimicking the patient's clinical signs. According to Berland et al. 2018, the water permeability of AQP4 is not affected by Ser111Thr mutation, in oocytes (Berland et al., 2018). Since AQP4 function depends on its proper localization at the astrocytic end-feet, and that it has a pro-inflammatory function, we

hypothesized that: Ser111Thr mutation leads to mislocalization of AQP4 and/or increased inflammation in the brain.

Importantly, the pathogenic Ser111Thr mutation leads to an interesting question about the non-channel functions of AQP4. Studying this mutation may give an insight into these non-channel functions, especially considering serine111 being a highly conserved residue in AQP4 (Berland et al., 2018).

In this project, the non-channel functions of AQP4 will be assessed. One of the non-channel functions is AQP4's pro-inflammatory role. Therefore, we study the extent of astrogliosis and microgliosis in the three respective regions: cerebellum hippocampus and parietal cortex were selected for investigation.

Cerebellum

The motor skills of the patient is highly affected and makes cerebellum important region to study due to its involvement in motor control and cognition (Koziol et al., 2014). Cerebellum, also termed as «little brain» contains Bergmann cells that form «tunnels» by surrounding a single purkinje neuron (Verkhratsky & Butt, 2007). Cerebellum is involved in execution of movement and cognitive functions (Brodal, 2004) and symptoms of injury or disease in that are area include gait ataxia. Considering that the patient has a gait disturbance, this region is important to investigate.

Hippocampus

Hippocampus is found in temporal lobe of the brain and is mainly divided in four main regions: Cornu Ammonia1-4 (CA1-A4). This brain region is involved in processing large amount of information due to its neocortical connections (Brodal, 2004). The patient exhibits mild intellectual disabilities, which make the hippocampus a relevant region to focus due to its association with development of intellectual cognitive skills and short-term memory (Brown & Aggleton, 2001; Latal et al., 2016).

Parietal cortex

Parietal cortex is one of the four major lobes in the brain involved in several process including cognition, motor and sensory – vision and hearing (Freedman & Ibos, 2018). The patient

exhibits some disturbance in the vision and hearing loss and parietal cortex was examined. The latter symptoms could be due to disturbances in the inner ear and retina, which are regions outside the scope of this master project.

All in all, selected brain regions correlate with phenotypes found in the patient and their abundant expression of AQP4.

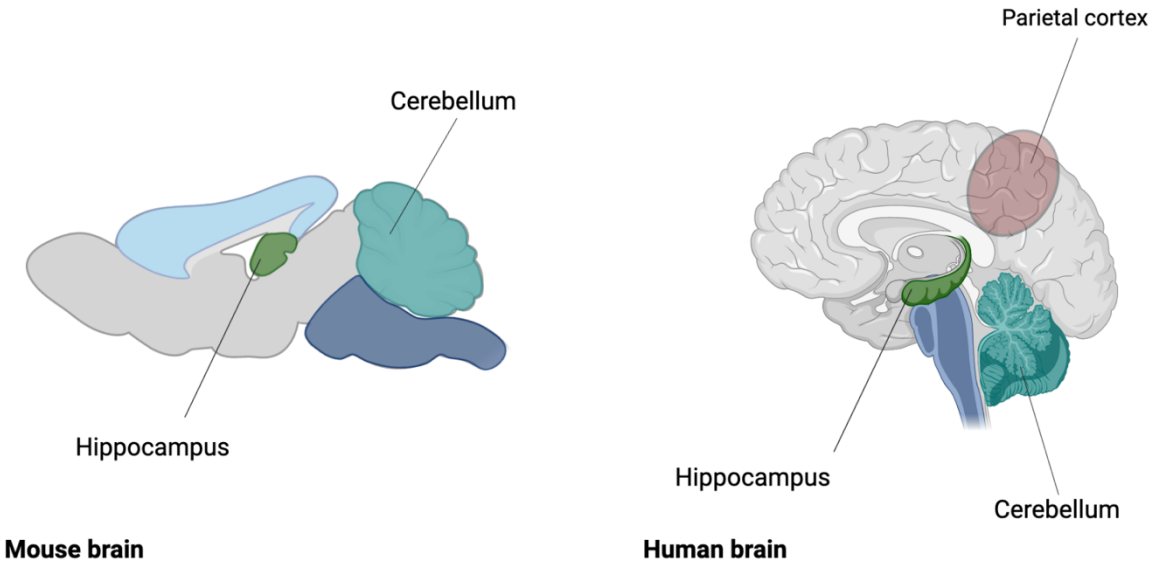

Figure 6: Midsagittal sections of mouse and human brain illustrating cerebellum, hippocampus, and parietal cortex. Cerebellum (light green) is located dorsal to the brain stem. Structurally, cerebellum constitute of specialized glial cells, termed Bergmann glia. These cells form a tunnel structure in cerebellum by surrounding a single purkinje neuron. Cerebellum is important for execution of movement and muscle coordination. The hippocampus (green) is found in the temporal lobe and divided in four regions: CA1, CA2, CA3 and CA4. It regulates important functions including short-term memory. Lastly, parietal cortex (red) is one of the four major lobes in brain and is mainly involved in sensory perception. Figure made in BioRender.com

We used immunoblotting, immunohistochemistry, and quantitative polymerase chain reaction (qPCR) to characterize the mutation. The goal of this project was to gain an understanding of the importance of the Ser111 residue in relation to the non-channel functions of AQP4.

2 Materials and methods

2.1 Developing an AQP4 S111T mouse model through gene modification

In order to investigate the S111T mutation, we generated transgenic animals through a widely used gene editing technique, known as Clustered Regulatory Interspaced Short Palindromic Repeats and CRISPR-associated protein 9 (CRISPR-Cas9). This technique is inspired by a genome editing system found in bacteria, to defend itself against bacteriophages (Jiang & Doudna, 2017). The system is based on two major components, a guide RNA and endonuclease referred to as Cas9. The guide RNA recognizes the specific sequence in the DNA that is further cleaved by Cas9. This system allows to alter the genome of animals, by inserting or deleting genomic DNA.

The CRISPR-Cas9 technique was used to generate an animal model of the pathogenic Ser111Thr missense point mutation. The mutation was generated by substituting serine at position 111 to threonine.

The pathogenic mutation found in the patient is a heterozygote missense mutation. To get a comprehensive overview of the effects of Ser111Thr AQP4 mutation in the mouse brain, we generated two different AQP4 genotypes in C57BL/6NRj mice (JANVIER laboratories, France) in collaboration with the Transgene Center at institute of Basic Medical Sciences at the University of Oslo.: heterozygote (wt/Ser111Thr) and homozygous (Ser111thr/Ser111thr) and compared these to wild type littermates.

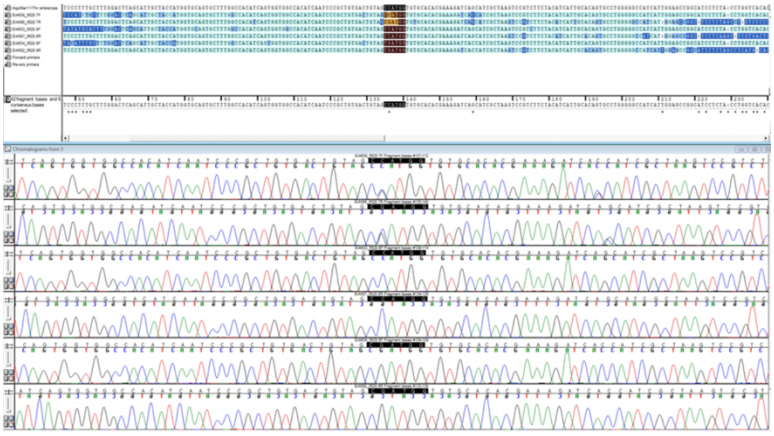

Figure 7: DNA sequencing chromatogram illustrating that experimental animals contains wanted mutation.

The table below gives an overview of number (n) of animals used for this project with their respective genotypes:

Table 1 – Number of animals and genotype used for immunohistochemical studies.

Genotype	Wild type (wt/wt)	Heterozygote (wt/S111T)	Homozygote (S111T/S111T)
Animals (n)	4	4	4

*wt= wild type, m = single mutation of Ser111Thr, mm= double mutation of Ser111Thr

Table 2 – Number of animals and genotype used for protein and transcript studies.

Genotype	Wild type (wt/wt)	Heterozygote (wt/S111T)	Homozygote (S111T/S111T)
Animals (n)	4	4	4

*Heterozygote and Homozygote of Ser111Thr mutation and their respective wild types

2.2 Experimental animals

Ethical consideration of experiment animals

All experiments conducted on animals were performed regard to guidelines approved by Norwegian food safety authority (NFSA). Everyone involved in handling and euthanasia of animals were certified for working with animals, which is required from NFSA. FOTS id of experimental animals used in this project; 12076.

2.2.1 Regional dissection of mouse brains

The regional dissection of parietal cortex (pcx), hippocampus (hc), and cerebellum (cb) were conducted. For protein analysis, twelve animals were used with their respective genotypes (n=4 per group). The animals were decapitated under isoflurane (Baxter, Deerfield, IL, USA) and the brains were dissected. The tissue from the brain regions were dissected out from both hemispheres. The tissues were snap frozen and stored in -80°C.

2.2.2 Perfusion-fixation of animals

To preserve the cytoarchitecture of the brain fixation perfusion was performed. Each animal was perfused and fixed with 4% paraformaldehyde (PFA) diluted in 0.1 M sodium phosphate (NaPi) buffer. The 4% PFA is used to fix tissues by preserving the structures of the proteins. The PFA attaches the molecules within the tissue by forming crosslinks between the molecules (Kim et al., 2017). Prior to perfusion, the animals were completely anesthetized by being injected with zirconium fluoride (ZRF). Once the animal was completely anesthetized, it was placed on a styrofoam platform for the surgical procedure and perfusion to take place. Prior to perfusion, the blood was rinsed with 2% dextran in 0.1 M NaPi by placing the perfusion needle in a 2% dextran solution thereby reversing the perfusion pump for 20 seconds. Further, the perfusion was conducted by inserting the perfusion solution in normal direction, consisting of the 4% PFA in 0.1 M NaPi, into the left atrium of the animal. An incision was made in the right atrium for the blood to drain out which inhibited pressure in the circulatory system during perfusion. By directly performing perfusion-fixation with a perfusion pump, the fixative solution is effectively distributed throughout the tissues (Au - Gage et al., 2012). After perfusion, the brain was taken out from the skull. The brain was fixed in 4% PFA overnight and further stored in 0.4 % PFA until cryostat sectioning.

2.3 Immunofluorescence and light microscopy

The immunofluorescence staining technique uses antibody as probes to detect specific structures within a cell or tissue. The detection is achieved by amplifying fluorescent dye, directly or indirectly, to the antibody.

Direct and indirect immunofluorescence

Antibodies or immunoglobulins (Ig) are glycoproteins which are specialized cells of the immune system. They act as a defense system by binding to foreign substances through antigens. Antibodies are widely used for immunohistochemistry studies which are harvested from various organisms.

The antibodies can be produced as polyclonal or monoclonal. The difference lies in the binding affinity of the antibodies to the epitopes. The surface of antigens consists of a highly specific

molecule called epitope, also referred to as antigenic determinant. For production of polyclonal antibodies, the organisms are injected with an antigen that result formation of antibodies from different immune cells and entails the antibodies to bind to multiple epitopes. In contrast, monoclonal antibodies have a high binding affinity toward one specific epitope (Buchwalow & Böcker, 2010).

For immunoassays, the antibodies are either directly or indirectly bound to the targeted molecule. The primary antibody is labelled with fluorescent dye and directly bind to the antigen of the molecule. This process is known to be direct. An indirectly labelling occur when fluorescent dye is labelled to a secondary antibody. This process is as follows, the primary antibody, without labelled dye, binds to a specific molecule. The secondary antibody, with labelled dye, binds to the primary antibody. The high labeling and detection sensitivity of the indirect labeling makes it the most common method used for immunodetection (Burry, 2009).

2.3.1 Tissue preparation for light microscopy

The perfusion fixed brains were cryo-protected in 10% for 2 hours, 20% for 2 hours and 30 % overnight. Soaking the brain in sucrose avoids formation of ice crystal formation in the tissue when cryosectioning. The brain was cut in midsagittal plane which divided the brain in left and right hemispheres. Each hemisphere was embedded in OCT for cryostat sectioning at -19°C. The thickness of the sections was 14 µm and the sections were collected on microscopic slides. Along the way, the sections were stained with crystal violet and observed under the microscope to confirm the tissue integrity. All slides were stored in -20°C until immunofluorescence staining experiments.

2.3.2 Immunofluorescence staining with AQP4, GFAP and Iba1

The sections were washed in 0.1 M phosphate buffered saline (PBS) for 3x5 minutes and further incubated for 1 hour with blocking solution, also known as pre-incubation solution. The sections were incubated with primary antibody solution diluted with primary antibodies. Incubation with primary antibodies was kept overnight at room temperature. The sections were washed 3x10 minutes in PBS and kept for incubation with secondary antibodies for 1 hour. The sections were again washed in PBS for 3x10 minutes. Lastly, the sections were incubated with

a nuclear stain (Hoechst 1:5000) for five minutes, and further washed in dH_2O for 3x5 minutes. The sections were mounted on glass slides with a coverslip for microscopic studies.

Table 3 – Primary and secondary antibodies with their respective concentrations used for staining aquaporin-4 (AQP4), astrocytes (GFAP), microglia (Iba1) and nucleus (Hoechst)

Staining	Primary antibody	Concentration	Secondary antibody	Concentration
AQP4	Rabbit anti-AQP4	1:500	Donkey Cy2	1:250
GFAP	Chicken anti-GFAP	1:500	Donkey Cy5	1:250
Iba1	Goat anti-Iba1	1:100	Donkey Cy3	1:250
Hoechst		1:5000		

2.3.3 Light microscopy imagining

Confocal microscopy (Zeiss, Jena, Germany) imagining was conducted on sagittal cryosections incubated with respective primary- and secondary antibodies. The images were collected with magnifications: 20x and 63x.

2.4 Protein analyses with Western Blotting

To identify the protein expression of AQP4 and other proteins of interest, immunoblotting was performed. Western blotting is considered a semi-quantitative method to analyze protein expression. Initially, proteins are separated according to their size or charge, through a technique called sodium dodecyl sulfate polyacrylamide gel electrophoresis (SDS-PAGE). For the identification of the protein of interest, a standard ladder is included which indicate the molecular weight (MW). Further, the proteins are transferred by Western Blotting to a membrane which makes the protein of bands visible after being labelled with a specific antibody (Mahmood & Yang, 2012).

2.4.1 Protein purification and western blot analysis

Sample preparation

For this project, proteins from cerebellum, parietal cortex, and hippocampus were extracted and used for experiments. These regions exhibit high AQP4 expression, and correlate with

phenotypes observed in the patient with Ser111Thr mutation. For each brain region (cb, hc and pcx) there was dissected twelve animals with their genotypes (wt/wt, wt/S111T, m/S111T, n=4 for each group).

For lysate preparation, twelve samples were prepared from each brain region. The brain tissues were dissolved in RIPA buffer and inhibitors such as phosphatase inhibitor cocktail PhosSTOP and protease inhibitor cocktail SigmaFAST, to prevent protein degradation. Each brain tissue was homogenized with respective amount of RIPA buffer and thoroughly vortexed. The samples were further kept on ice for 30 minutes and centrifuged at 14000 rpm at 4°C for 15 minutes. The supernatant containing solved protein was collected.

Estimation of Protein concentration

Pierce™ bicinchoninic acid (BCA) protein assay kit (Thermo Fisher Scientific, USA) was used to perform for quantitation of proteins. A microplate was prepared and proteins with 1:10 dilution of RIPA buffer and added into each well. Duplicate of samples were included. Lastly, 200 µl BCA standard solution was added in each well. The microplate was kept for incubation at 37°C for 30 minutes.

After incubation, the concentration of protein samples is estimated by measuring the absorbance with a spectrometer. The spectrometer collected all the data and resulted a BCA standard curve with a linear range of proteins.

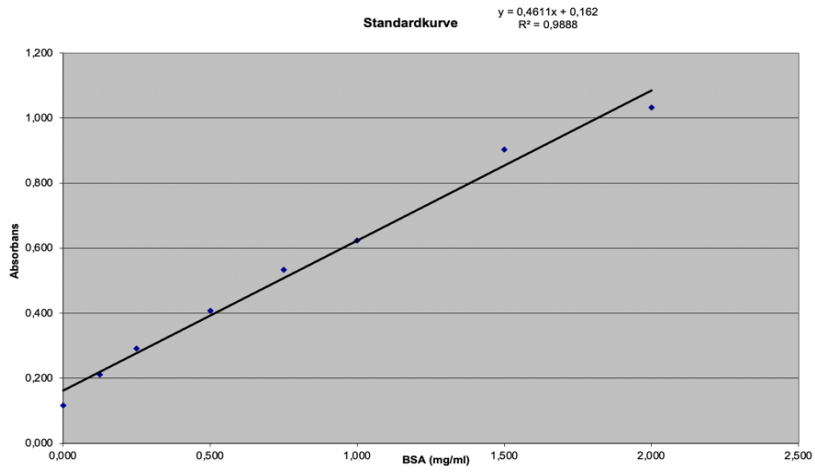

Figure 8: BCA standard curve with linear range of protein. The protein concertation (x-axis) and its absorbance (y-axis) spotted on the graph. The highest protein concertation measured in the standard curve is 2,0 mg/ml. $R^2 = 0.9888$

Sodium dodecyl sulphate-polyacrylamide gel electrophoresis (SDS-PAGE)

Loading buffer (LB) was added into protein samples, which consist of a dye that visualize the protein migration during electrophoresis. In addition, it consists of β-mercaptoethanol breaks down the disulfide band (S-S) and denatures the proteins structure. After adding the LB, the samples heated at 37°C for 10 minutes. Polyacrylamide gels (4-20% and 10%) (BioRad, Hercules, California, USA) was used for all experiments. The gel was placed in a gel-apparatus filled with 1x Laemmli running buffer. Prior to protein loading, the wells were rinsed to prevent bubbles. The wells were loaded with 10 µl of samples and a standard solution was included. Further, for the separation of proteins the gel was run with a voltage at 160 V for 60 minutes until the dye ran to the bottom.

Blotting

The aim of blotting is to transfer proteins from the gel to a hydrophilic polyvinylidene fluoride (PVDF) membrane. After SDS, a blotting «sandwich» is created. The PDVF membrane was activated with 100% ethanol/methanol, and further placed in Towbin blotting buffer. The PVDF membrane is, carefully, placed on the gel and ensure to prevent any air bubbles. The membrane is covered with three filter papers and a blotting pad. Finally, the blotting «sandwich» is placed in a blotting chamber. An ice pack and a magnet are placed in the chamber and filled with 1x transfer blotting buffer. The blotting was run with a voltage of 100V for 30 minutes.

Immunodetection

The membrane was again activated in 100% methanol/ethanol for Ponceau S staining. The Ponceau S staining is suitable for visual inspection of the blotting. The solution was added, to the membrane, for approximately one-minute and washed with water until the bands are visible. For immunodetection, the membrane was blocked with 5% Bovine Serum Albumin (BSA) for 1 hour. After blocking, the membrane was rinsed with TBST and further incubated with primary antibody (1 ml 5% BSA + 4 ml TBST) overnight. Next, the membrane was incubated with secondary antibody (1 ml 5% BSA + 4ml). Furthermore, the membrane was washed 3x10 minutes with TBST and developed with SuperSignal, West Pico (Thermo Scientific) for 5 minutes. For imaging a BioRad Touch ChemiDoc digital imaging system was used.

2.4.2 Densitometric analysis

Prior to statistical analysis, the signal intensity of immunoblots were measured with Image Studio Lite software version 5.0. The signal intensities of the protein of interest were divided with its respective housekeeping control band signal intensity for normalization. Group averages were used for statistical analysis, and numbers are presented as percentages of the average WT control values. Statistical analysis was performed with SPSS version 27 using Analysis of variance (ANOVA) along with LSD post hoc test. The values are presented as mean ± and standard error is included. A p-value < 0.05 was considered as significant. GraphPad Prism 9 (San Diego, USA) was used to create graphs.

2.5 mRNA transcript analysis with RT-qPCR analysis

2.5.1 RNA isolation from brain tissues

Samples from cerebellum, hippocampus and parietal cortex were prepared. The samples were homogenized with a lysis buffer consisting of phenol and guanidine isothiocyanate that lyses the cell membranes to access the RNA. After homogenization, the samples were centrifuged for 3 minutes at maximum speed. The supernatant was removed and transferred to a genomic DNA (gDNA) eliminator spin column (QIAGEN, Hilden, Germany). The lysate was centrifuged for 30 seconds at maximum speed thereby flow-through was collected. For RNA isolated there was used Rneasy plus mini kit (QIAGEN, Hilden, Germany). One volume of 70% ethanol was added to the flow-through and loaded into a RNeasy spin column. It consists of silica gel membrane which isolates the RNA molecules while eluting the remaining structure. The centrifugation was performed for 15 seconds at maximum speed, the flow-through was discarded. The samples were washed with RW1 washing buffer and thereby centrifuged for 15 seconds at maximum speed. During this step, the remaining contaminants bounded to the silica gel membrane are removed, only RNA molecules are bound to the membrane. The flow-through was discarded and the samples were again washed with a mild washing RPE buffer and thereby centrifuged for 2 minutes at maximum speed. Optionally, the samples were centrifuged dry for one minute at maximum speed. The RNeasy spin column, containing RNA, was placed into a new tube, and eluted with RNeasy free water. Lastly, centrifugation was performed for one minute at maximum speed. The water isolates the RNA by loosening the RNA molecules from silica membrane. The flow-through, containing the RNA, was collected for synthesis of

complementary DNA (cDNA). Prior to the cDNA synthesis, the concertation and purity of RNA samples was measured with Nanodrop® spectrophotometer (Thermo Scientific, Waltham, Massachusetts, USA).

2.5.2 cDNA synthesis from total RNA

The synthesis of cDNA from RNA was performed by using GoScript™ Reverse Transcription System (Promega, Madison, WI, USA).

To begin with, we prepared 500ng RNA from each sample, and combined with Oligo dt15 primer and Nuclease-Free water to ensure equal volumes across samples. The samples were heat blocked at 70ºC for 5 minutes and cooled on ice. A mastermix containing reverse transcriptase enzyme (Promega, Madison, WI, USA) was added to the heat blocked samples and cDNA synthesis was performed. For annealing, the reaction samples were kept at 25ºC for 5 minutes and extension was performed at 42ºC in a thermocycler for one hour. Prior to RT-qPCR, the reverse transcriptase was inactivated by heat block at 70ºC for 15 minutes.

2.5.3 Real-time quantitative polymerase chain reaction – qPCR

The Quantitative polymerase chain reaction (qPCR) is method used for quantitative analysis of gene expression. It differs from the regular PCR by quantifying amplified DNA after each cycle while regular PCR detect the amount of DNA at the end of the reaction (Jalali et al., 2017). During qPCR assay, the amplification of DNA is measured and differences in gene expression level is quantified (Taylor et al., 2010). For this project, we performed SYBR Green based qPCR for detection of the genes of interests: *Aqp4*, *Gfap, Iba1* with gene name *Aif-1,* and microglia markers (*Itgam, Cd14, Cxcl10, Cx3cr1*). The SYBR green consist of fluorescent dye which interact with DNA bases and the technology is based on two hybridization events, that are forward and reverse primers.

The qPCR reaction is directed by a thermocycler which requires optimal conditions for a successful DNA amplification. There are three major steps in qPCR where the first step is denaturation, the DNA is heated with 95°C. During this process the double helix is separated into single-stranded DNA. The second step is annealing, the temperature is decreased to 60°C. The respective primers are annealed to the single stranded DNA thereby synthesize a new

strand. The last step is elongation, the temperature is heated to 72°C. The DNA is synthesized by thermostable polymerase that adds the dNTPs and extends the newly synthesized DNA.

2.5.4 qPCR reaction preparation

There was performed SYBR Green based qPCR analysis on samples from cerebellum, parietal cortex, and hippocampus. The samples were loaded in the wells of a microplate. master mix solution was added into each well containing power SYBR Green PCR Master mix (Applied Biosystems, Oslo, Norway), forward primers (10 uM) and reverse primers (10uM) and cDNA. In addition, no template control (NTC) was included as negative control. A schematic illustration of the plate set-up is shown in figure 9. Thermal cycler from StepOnePlus system (Applied Biosystems) was used for qPCR reaction.

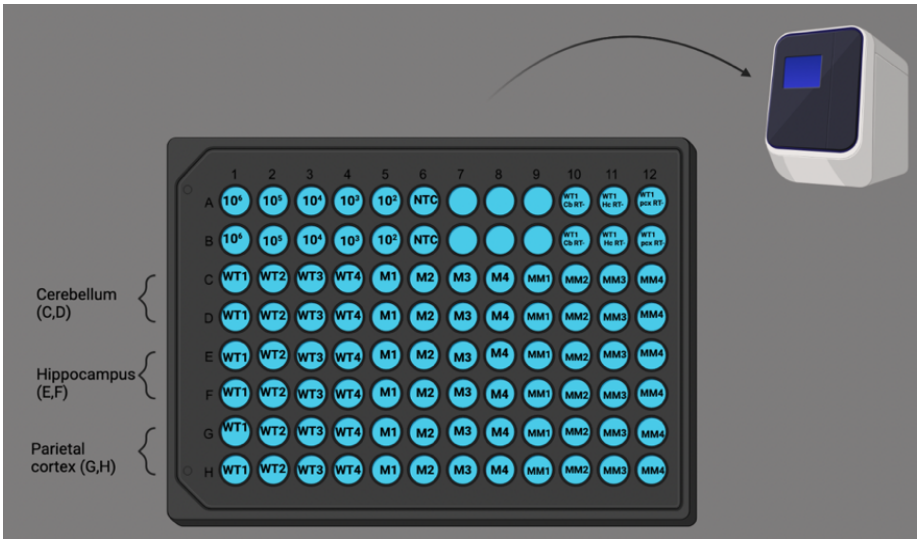

Figure 9: Schematic illustration of microplate set-up for qPCR machine. Cerebellum, hippocampus, and parietal cortex samples with genotypes (wt/wt, wt/S111T and S111T/S111T). Duplicate from each sample was included. The transcript mRNA levels of AQP4, GFAP, Iba1 and microglia markers were analyzed. No control template (NTC) was included. The DNA was amplified in in optimal conditions, by PCR. Figure made in BioRender.com

Table 4 – Genes and respective forward and reverse primer sequences

Gene Name	Forward Primer	Reverse Primer
Aqp4	AGCAATTGGATTTTCCGTTG	TGAGCTCCACATCAGGACAG
Aif1	CTGCCAGCCTAAGACAACCA	GGAATTGCTTGTTGATCCCCT
Gfap	GCACTCAATACGAGGCAGTG	GCTCTAGGGACTCGTTCGTG
Cx3cr1	TGCTCAGGACCTCACCATGTC	CTCAAGGCCAGGTTCAGGAG
Itgam	TGCGCGAAGGAGATATCCAG	GCCTGCGTGTGTTGTTCTTT
Cd14	CAGAGAACACCACCGCTGTA	CACGCTCCATGGTCGGTAGA
Cxcl10	ATGACGGGCCAGTGAGAATG	TCGTGGCAATGATCTCAACAC
Ubc	CGTCGAGCCCAGTGTTACCACC AAGAAGG	CCCCCATCACACCCAAGAACA AGCACAAG

**Aif1= iba1*

2.5.5 Analysis of qPCR data

The NormFinder software (Aarhus, Denmark), was used to analyze the stability of the gene expression. To determine the correct housekeeping gene, set of various genes were analyzed: *Ubc, H2afz* and *Pgk1*. The *Ubc* gene was selected due its stability compared to other genes. For statical analysis, we used SPSS version 27 and one-way ANOVA along with LSD post hoc test. Group averages was used for the statistical analysis. The values are presented as mean ± and standard error is included. A P-value < 0.05 was considered as significant.

3 Results

Although a functional study of the pathogenic S111T-AQP4 shows that the water permeability is not affected by the mutation. (Berland et al., 2018), the focus in this project is to give a molecular characterization of S111T-AQP4 mutation. For the first time, non-channel functions of S111T-AQP4 will be assessed. Both protein- and mRNA transcript levels of AQP4 were investigated to see if the S111T/S111T mutation affects the AQP4 expression. There was performed immunoblotting and RT-qPCR analysis. Our hypothesis implies that the localization of AQP4 might be affected by S111T-AQP4 mutation. To see if the mutation influences the distribution of AQP4 in the brain, immunofluorescence staining on sagittal brain sections was performed. The expression and subcellular localization of AQP4 with Ser111Thr mutation was investigated in two genotypes for immunofluorescence experiments (WT vs S111T/S111T) and all three genotypes for protein and qPCR analysis (WT, WT/S111T, and S111T/S111T). The regions investigated were cerebellum, parietal cortex, and hippocampus.

To answer our hypothesis regarding inflammation caused by S111T-mutation, we investigated GFAP and Iba1 on protein and mRNA transcript levels, to see if they initiate a pro-inflammatory response of AQP4 in the brain. Important microglial markers which are important for microglial activation, were also investigated on mRNA transcript level. Along with AQP4 IF staining, the distribution of GFAP and Iba1 was observed under light microscope with magnifications; 20x and 63x.

3.1 Immunofluorescence localization of AQP4, GFAP and Iba1 in WT vs S111T-AQP4 animals

The expression and cellular localization of proteins of interest; AQP4, GFAP and Iba1 was investigated in cerebellum, hippocampus, and parietal cortex from animals with each genotype; WT/WT, WT/S111T and S111T/S111T. Observation of AQP4 expression was investigated nearby the astrocytic end-feet where they contribute to form perivascular processes and close to neuropil where synaptic activation occurs.

Taken into consideration that homozygous mutation will lead to severe phenotypes than heterozygous, therefore only two genotypes; WT and S111T/S111T animals were included in immunofluorescence analysis and to investigate the subcellular distribution of AQP4 in the

respective brain regions. In addition, to investigate neuroinflammatory response of S111T-AQP4, the astrocyte marker GFAP and microglia marker Iba1 was included in the analysis. The images, taken by light microscope (Zeiss, Jena, Germany) with 20x and 63x magnification to gain overview of the distribution.

3.1.1 Localization of AQP4 in WT and S111T/S111T-AQP4 mice brain

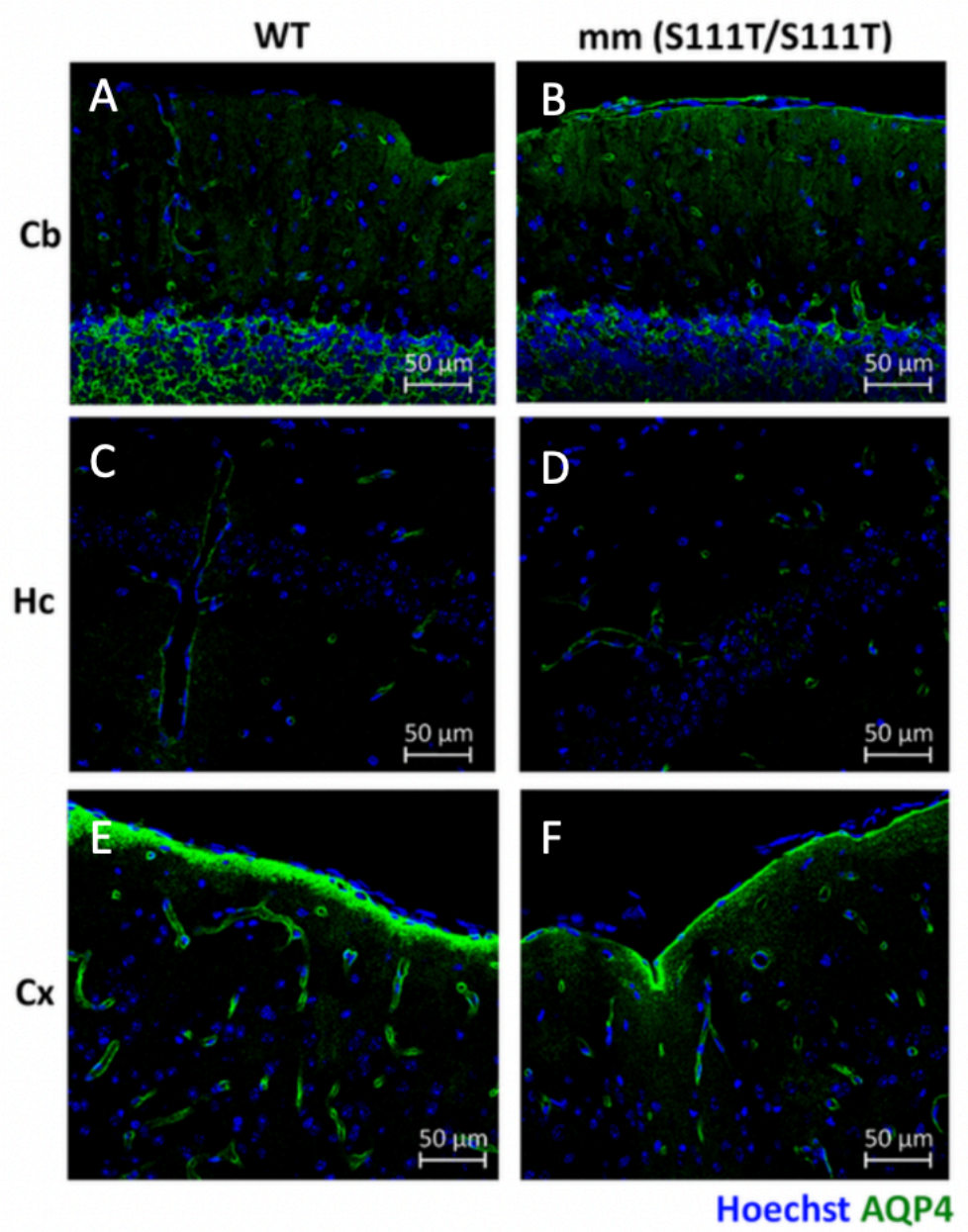

Figure 10 – Localization of AQP4 in WT and S111T/S111T-AQP4 mice brain. Immunolocalization of AQP4 (green) is shown at the astrocytic end-feet surrounding blood vessel in all regions in both genotypes of mice brains. Bergmann glia in the Purkinje layer of cerebellum show dense AQP4 labelling, in both genotypes **(a, b)**. In cortex AQP4-labeling is strong near subpial membranes, in WT and mutated animals **(e, f)**. No visible differences are observed between the genotypes. Co-staining of Hoechst (blue) visualize nuclei in mice brain. Images are obtained with 20x magnification. Scale bar = 50 µm.

Figure 10 shows AQP4 (green) and co-staining of Hoechst (blue) labeling in cerebellum, hippocampus, and parietal cortex. IF staining showed an overview of localization and distribution of AQP4 in the three brain regions. The expression of AQP4 is highly concentrated at perivascular end-feet abutting blood vessels and dense expression is observed in the subpial membranes, mainly in cortex (Figure 10). Restricted expression of AQP4 is represented nearby neuropil that is found nearby nuclei (blue).

Involvement of IF staining, which is semi-quantitative method, was important to consider for gaining an insight into the subcellular localization and distribution of AQP4 in the brain. While the figure suggests weak labeling of AQP4 in S111T/S111T in cerebellum compared to wild type, we performed a blind test of each section, which confirmed that AQP4 expression seemed unchanged in S111T/S111T-animals compared to wild type. This might be due to the intensity of fluorescent labeling varying between the sections.

Overall, AQP4 expression does not show any changes between two genotypes in cerebellum, hippocampus, and parietal cortex.

3.1.2 Extent of astrogliosis judged by GFAP immunofluorescence staining of brain from WT and S111T/S111T-AQP4 mice

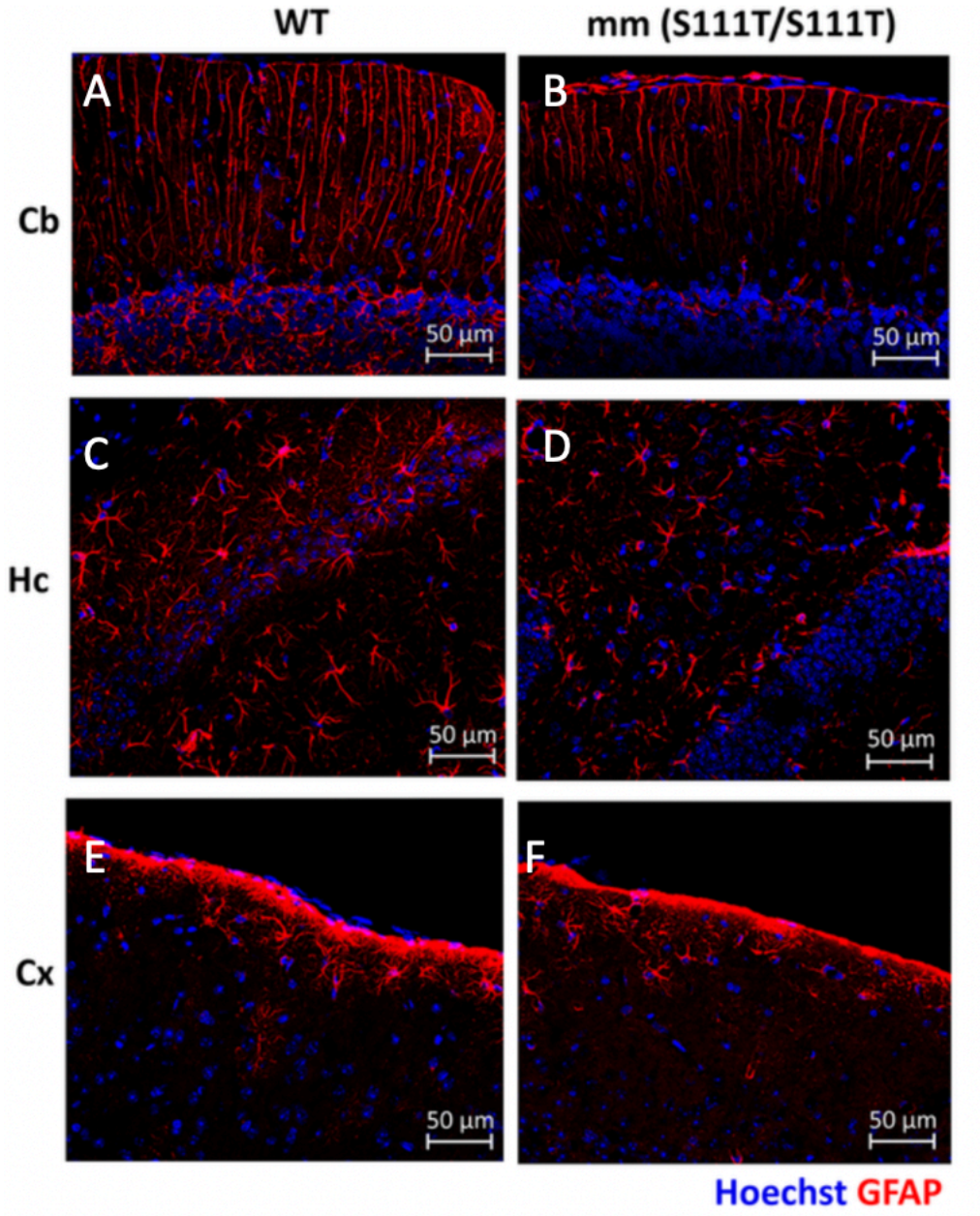

Figure 11 – Extent of astrogliosis judged by GFAP immunofluorescence staining of brain from WT and S111T/S111T-AQP4 mice. Immunolocalization of GFAP (red) is shown in WT and S111T/S111T. In both genotypes, the Bergmann glia processes are extending to the subpial membranes in cerebellum **(a, b).** The CA1 region of hippocampus is focused to show GFAP in both genotypes **(c, d)**. Dense expression of GFAP (red) is shown at the subpial membrane in cortex in both genotypes **(e, f)**. No visible changes are found in expression of GFAP between the genotypes. Co-staining of Hoechst (blue) labelling visualize the nuclei. Images are obtained 20x magnification. Scale bar = 50 µm.

It is has been shown that AQP4 facilitates a pro-inflammatory response during pathological conditions (Prydz et al., 2020). GFAP is often used as a marker for reactive astrocytes involved in neuroinflammation.

Immunolocalization of GFAP was investigated to see if the pathogenic S111T-AQP4 mutation facilitates inflammation. In both genotypes, GFAP staining was observed in cerebellum, hippocampus, and cortex. In cerebellum, both genotypes show the long Bergmann glial processes that reaches to the subpial membranes. A dense expression of astrocytes was observed in the subpial membranes of cortex, respectively in both genotypes. The CA1 region of hippocampus was focused due to its involvement in important processes and is also affected during MTLE pathogenesis (Eid et al., 2005). The distribution of GFAP in CA1 remains the same in both genotypes. Our results indicate there were no noticeable changes of GFAP-labeled astrocytes observed in the three brain regions (Figure 11).

3.1.3 Assessment of microglia judged by Iba1 immunostaining in brain from WT and S111T/S111T-AQP4 mice

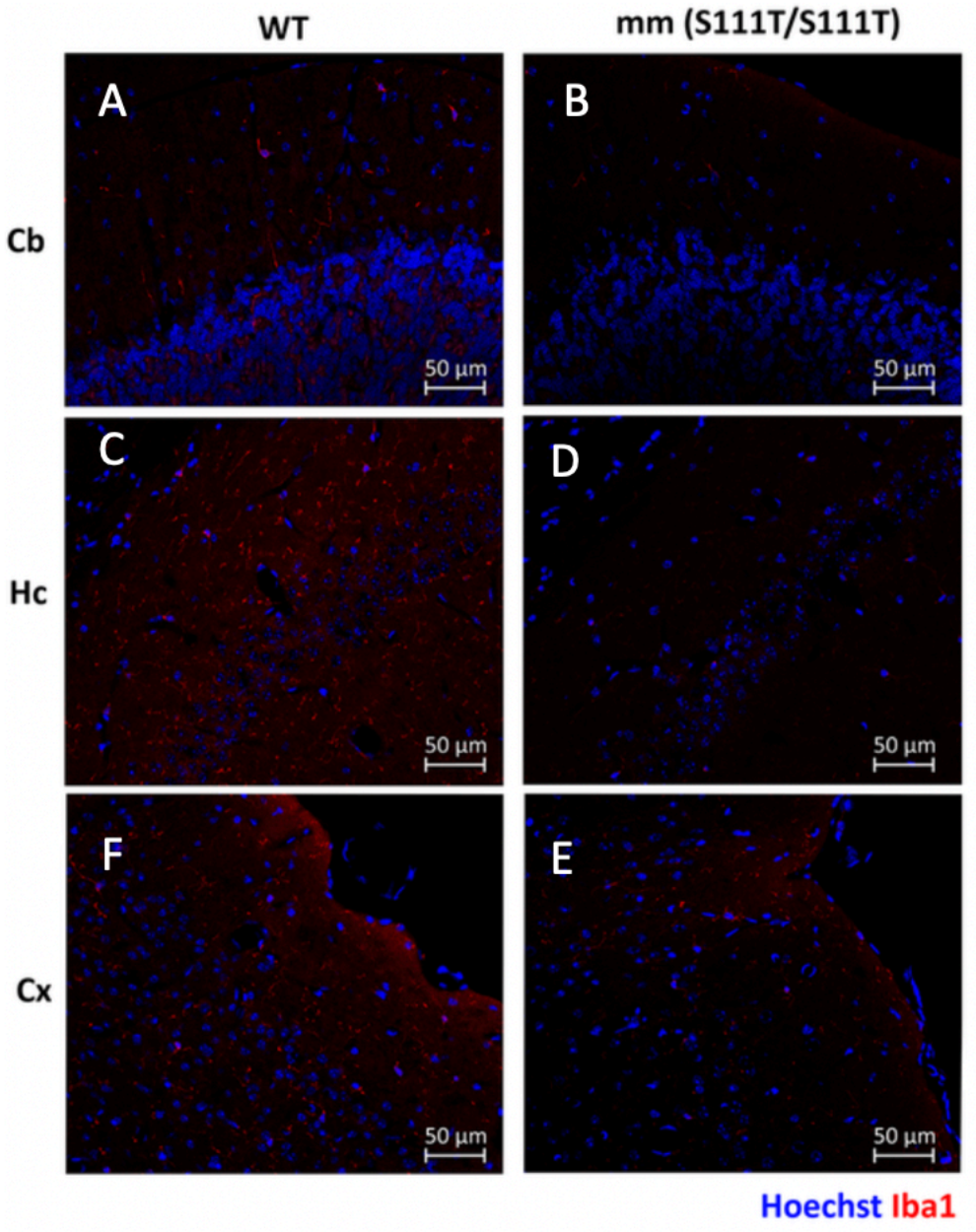

Figure 12 – Assessment of microglia judged by Iba1 immunostaining in brain from WT and S111T/S111T-A1P4 mice. Immunolocalization of microglia (red) is shown in the three brain regions. Fewer Iba1-labeled positive microglia is shown in all the three regions of the S111T/S111T-animals **(b, d, e)** compared with the WT. In cortex, there is possible to see some labeling of Iba1 but strong enough. Co-staining of Hoechst (blue) is included. Images are obtained from 20x magnification. Scale bar = 50 µm.

3.1.4 Iba1-positive cells in brain of WT-AQP4 and S111T/S111T-AQP4 mice

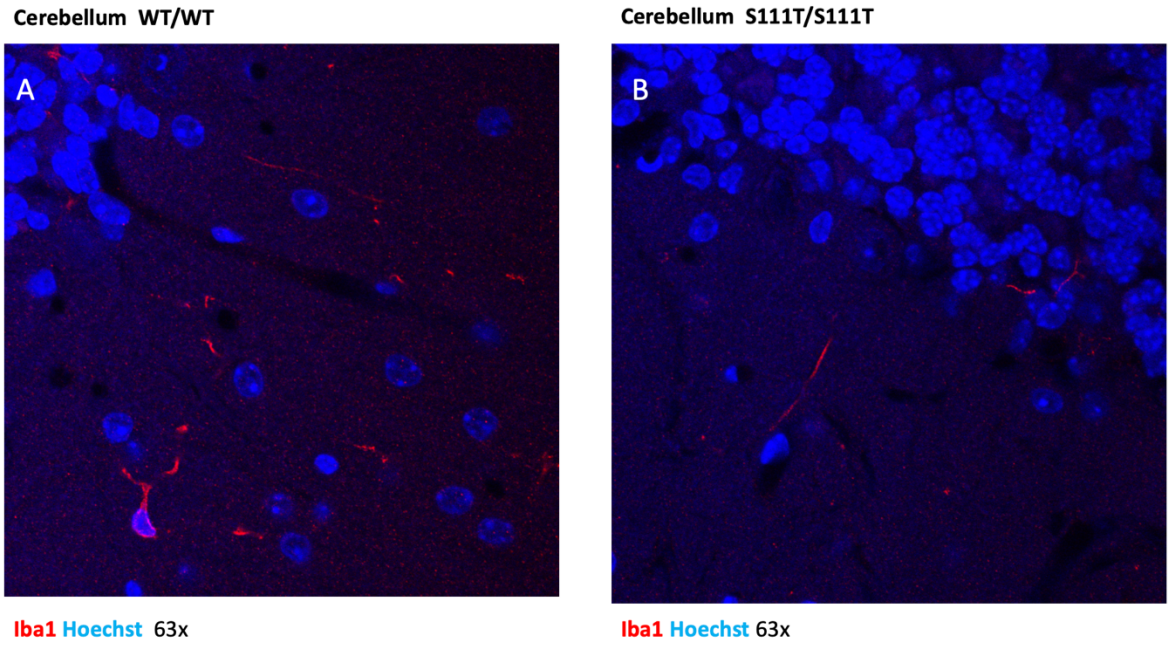

Figure 13 – Iba1-positive cells in brain of WT-AQP4 and S111T/S111T-AQP4 mice. Immunolocalization of Iba1-labeled microglia (red) are investigated with 63x magnification, only in cerebellum. Showing there is positive microglia expressed in both genotypes. Co-staining of Hoechst (blue) is included. Images are obtained from 63x magnification.

Ionized calcium-binding adaptor protein-1 (Iba1) was used to detect microglia in the brain. Iba1 is expressed in both resting and activated microglia, which makes it a specific marker to detect microglia activity during healthy brain and inflammation (Hopperton et al., 2018). Immunostaining of the brain sections with Iba1 showed Iba1 positive microglia across all the three regions investigated in both the genotypes (Figure 12 and 13). There was observed fewer Iba1 positive microglia in all brain regions of S111T/S111T-animals (figure 12). To confirm the presence of microglia in S111T/S111T animals, we performed imaging at 63x magnification only in cerebellum (Figure 13). The results actively indicate that microglia are present in both genotypes. Qualitatively, we observed a tendency towards less microglial labeling in S111T/S111T animals compared to wild type.

3.2 Ser111Thr mutated AQP4: AQP4 expression on protein and mRNA level

3.2.1 AQP4 is decreased on the protein level in cerebellum of S111T/S111T animals, while an unknown high molecular weight AQP4 positive band is observed

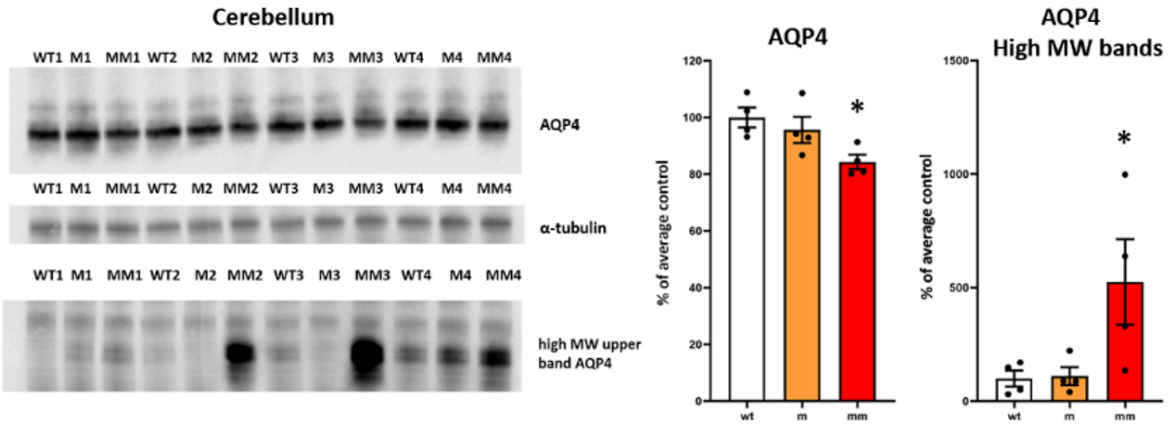

*Heterozygous mutation= m and homozygous mutation = mm

Figure 14 – AQP4 is decreased on the protein level in cerebellum of S111T/S111T animals, while an unknown high molecular weight AQP4 positive band is observed. (A) Immunoblot assessment of AQP4 protein lysates shows decreased AQP4 on the protein level only in S111T/S111T animals. A higher molecular weight band is especially apparent in S111T/S111T animals. (B-C) Densitometric analysis of the immunoblots confirms significantly downregulated AQP4 compared to WT cerebellum (B), while the high molecular weight bands are significantly upregulated (C). *Sig ANOVA LSD post hoc test; error bars: SEM; $P < 0.05$; $n = 4$

Cerebellum

Immunoblotting of AQP4 in cerebellum resulted AQP4 bands with a molecular weight of ~ 37 kDa. In addition, there was observed higher bands of AQP4 which had molecular weight of ~200 kDa. The higher molecular weight bands were observed a dramatically larger extent in the homozygous mutation (specially mm2, mm3 and mm4) of AQP4, possibly indicating AQP4 protein aggregates in this genotype. α-tubulin (50 kDa) was used as housekeeping protein to normalize the expression of AQP4 in the cerebellum. The densitometric analysis revealed a significant decrease of AQP4 in homozygous mutation compared to wild type. In addition, analysis from the higher bands resulted significant increase of AQP4 (~200 kDa) in homozygous mutation compared with both wild type and heterozygous mutation. The higher

molecular bands of AQP4 (~200 kDa) are most prominent in animals with S111T/S111T mutation. Simultaneous, the downregulation of AQP4 expression is also found in the same animals with that genotype. The aggregation of AQP4 in this genotype may indicate AQP4 binding to a higher molecule caused by the S111T/S111T mutation.

3.2.2 AQP4 in parietal cortex and hippocampus are not significantly altered on the protein level

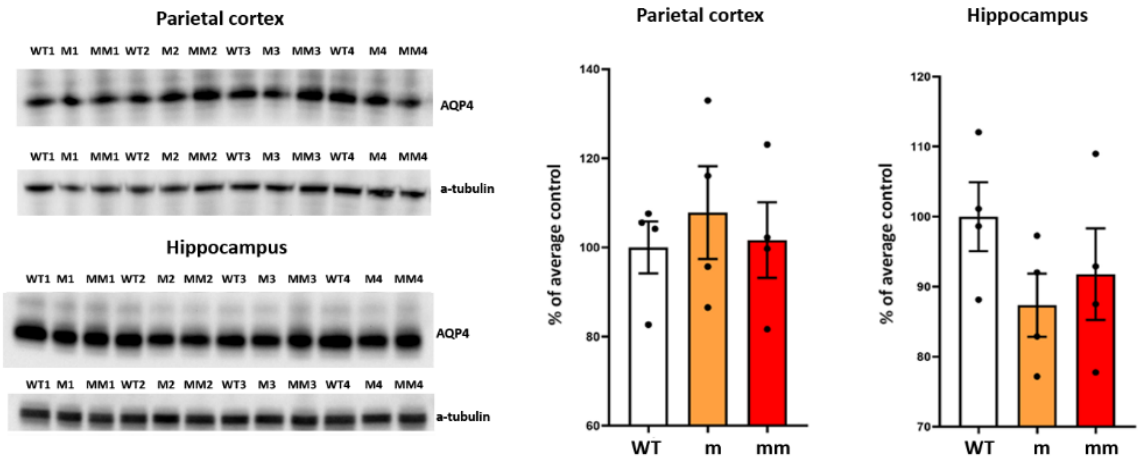

*Heterozygous mutation= m and Homozygous mutation = mm

Figure 15 – AQP4 in parietal cortex and hippocampus are not significantly altered on the protein level. Immunoblot assessment of AQP4 protein lysates shows no change in AQP4 expression on the protein level, in both brain regions. *Sig ANOVA LSD post hoc test; error bars: SEM; P > 0.05; n = 4

Parietal cortex and hippocampus

Immunoblotting assessment of AQP4 (37 kDa) in parietal cortex and hippocampus was conducted. The expression of AQP4 was normalized with α-tubulin (50 kDa). Densitometric analysis did not show significant changes of AQP4 expression between the genotypes, showing that expression of AQP4 at protein level is not altered by the mutation in between the genotypes.

3.2.1 AQP4ex is decreased on protein level in cerebellum of S111T/S111T animals

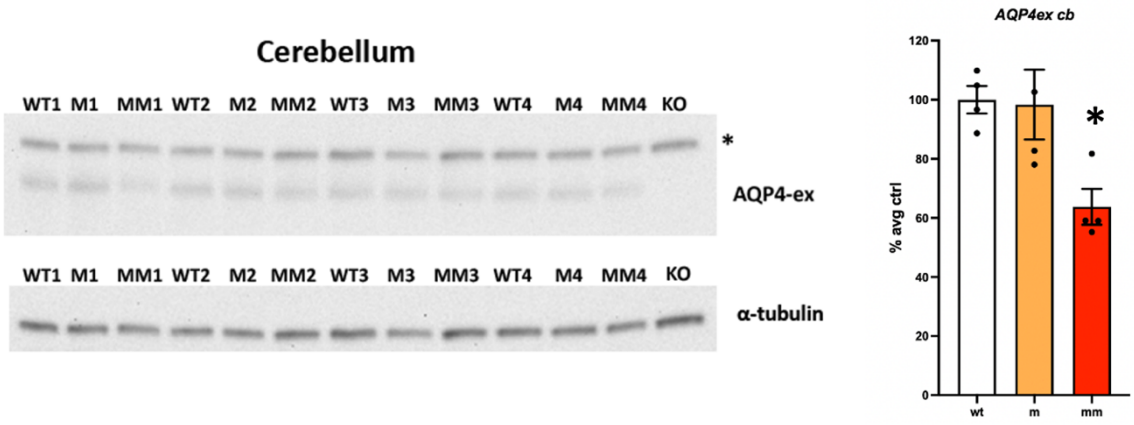

*Heterozygous mutation = m and homozygous mutation = mm

Figure 16 – AQP4ex is decreased on protein level in cerebellum of S111T/S111T animals. Immunoblot assessment of AQP4ex shows decreased AQP4ex on protein level only in S111T/S111T animals. AQP4-KO is included to determine the non-specific bands (*). Densitometric analysis of the immunoblots confirms significantly downregulated AQP4ex compared to both genotypes. *Sig ANOVA LSD post hoc test; error bars: SEM; $P < 0.05$; $n = 4$

To investigate the downregulated AQP4 in cerebellum there was performed immunoblotting analysis of AQP4ex, which is necessary for AQP4 anchoring in the plasma membrane. Densitometric analysis of AQP4ex immunoblots confirms AQP4ex is decreased on protein level in cerebellum of S111T/S111T animals. Figure 16 shows, together with AQP4ex (35 kDa) bands, non-specific bands were observed with a molecular weight of 37 kDa. identical as AQP4. To investigate the unknown bands there was included AQP4-KO lysate, labeled as «KO» (Figure 16). AQP4-KO was included to show if the bands are an isoform of AQP4, since it resulted same molecular weight as AQP4. The lysate with AQP4-KO still resulted a non-specific band concluding that the bands do not include AQP4.

AQP4ex isoform constitutes 10% of AQP4 and shows to be important for its anchoring (Palazzo et al., 2019). The highest expression of AQP4ex was found in the cerebellum compared to other brain regions, which is consistent with the finding shown in the study done by Palazzo et al 2019 (Palazzo et al., 2019). Interestingly, similar changes in AQP4ex expression were not seen in hippocampus or parietal cortex. The downregulation of AQP4ex of S111T/S111T animals suggests that protein level of AQP4ex in cerebellum is most affected, which may indicate importance of the serine residue during AQP4 anchoring in cerebellum.

3.2.2 *Aqp4* is increased on transcript mRNA level in cerebellum and hippocampus of S111T/S111T animals

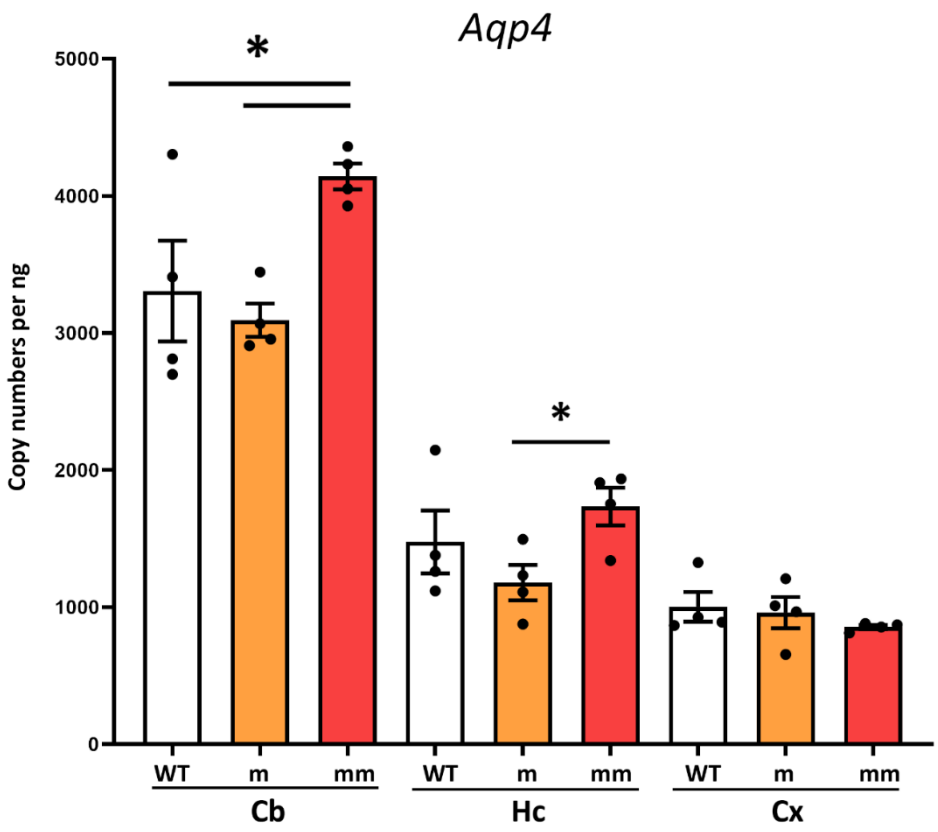

*Heterozygous mutation = m and homozygous mutation = mm

Figure 17 – *Aqp4* is increased on transcript mRNA level in cerebellum and hippocampus of S111T/S111T animals. Quantitative-PCR analysis of S111T/S111T animals shows an increased transcript mRNA expression in cerebellum and hippocampus, while transcript of *Aqp4* in parietal cortex is unaltered. Densitometric analysis confirms significantly upregulated *Aqp4* transcript expression in cb compared to WT and WT/S111T. Upregulated *Aqp4* transcript mRNA in Hc is also observed compared to only WT/S111T. *Sig ANOVA LSD post hoc test; error bars: SEM; $P < 0.05$; $n = 4$

For the investigation of the mRNA levels of *Aqp4* in the respective brain regions we performed qPCR analysis from cerebellum showed significant increase in *Aqp4* transcript levels in homozygous mutation compared with both wild type and heterozygous mutation. In addition, in hippocampus there was observed a significant increase in *Aqp4* on transcript level in homozygous mutation compared with heterozygous mutation. Parietal cortex showed no significant changes in *Aqp4*expression on transcript level. The data obtain suggest that mRNA levels of *Aqp4* in cerebellum and hippocampus are altered in S111T/S111T animals.

3.3 Ser111Thr mutated AQP4: GFAP expression

3.3.1 GFAP is increased on protein level in parietal cortex of S111T/S111T animals

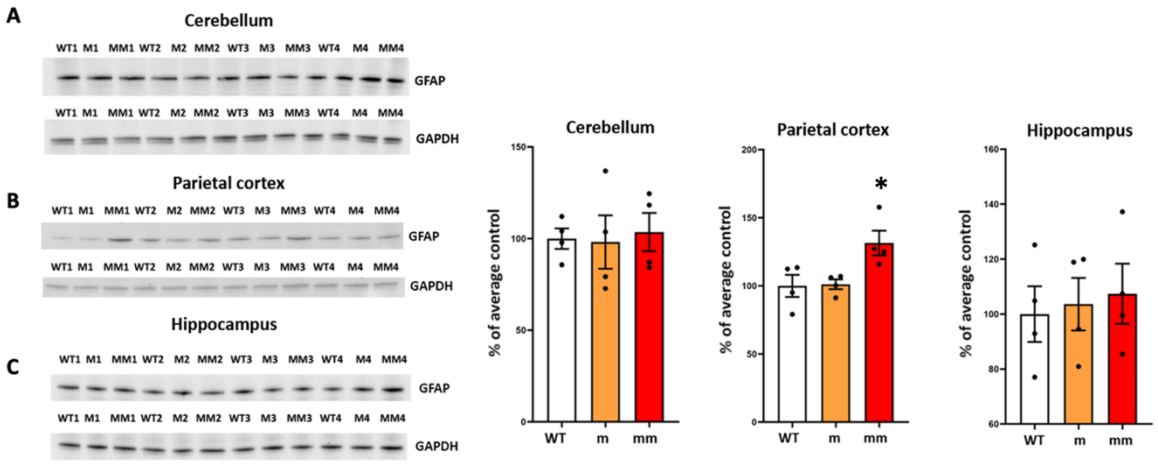

*Heterozygous mutation = m and homozygous mutation = mm

Figure 18 GFAP is increased on protein level in parietal cortex of S111T/S111T animals. B) Immunoblot assessment of GFAP (~50 kDa) in parietal cortex shows upregulated GFAP only in S111T/S111T animals. The expression of GFAP was normalized with GAPDH (~36 kDa). Densitometric analysis of the immunoblots confirms significantly upregulated GFAP compared to two genotypes. *Sig ANOVA LSD post hoc test; error bars: SEM $P < 0.05$; $n = 4$.

The expression of astrocytes was investigated due to their neuroinflammatory response during pathological conditions. To investigate the protein levels of astrocytes, immunoblot assessment of GFAP (~50 kDa) in cerebellum, parietal cortex and hippocampus was performed in the respective regions. Glyceraldehyde 3-phosphate dehydrogenase (GAPDH) (36 kDa) was selected as housekeeping protein. Figure 18 shows significant upregulated GFAP on protein levels only in parietal cortex which suggest that the parietal cortex of S111T/S111T animals is the only region affecting GFAP expression on protein level. It may also indicate that an inflammation in this brain region is in progress.

3.3.2 Transcript mRNA levels of *Gfap* in cerebellum, hippocampus, and parietal cortex remains unchanged

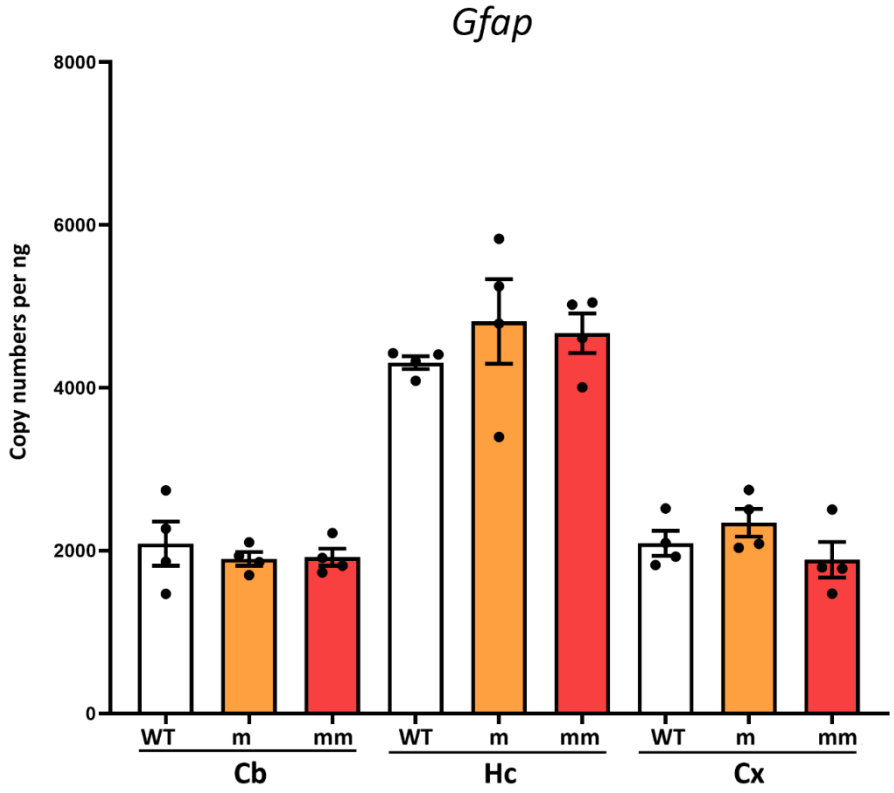

*Heterozygous mutation = m and homozygous mutation = mm

Figure 19 Transcript mRNA levels of *gfap* in cerebellum, hippocampus, and parietal cortex remains unchanged. qPCR analysis and densitometric analysis of mRNA levels in cerebellum, hippocampus, and parietal cortex with respective genotypes did not show significant changes. *Sig ANOVA LSD post hoc test; error bars: SEM; P > 0.05; n = 4

Quantitative-PCR analysis showed that transcript levels of *Gfap* in cerebellum, hippocampus and parietal cortex is not significantly changed between the genotypes.

3.4 Ser111Thr mutated AQP4: Iba1 expression

3.4.1 Iba1 is decreased on protein level in cerebellum of S111T/S111T animals

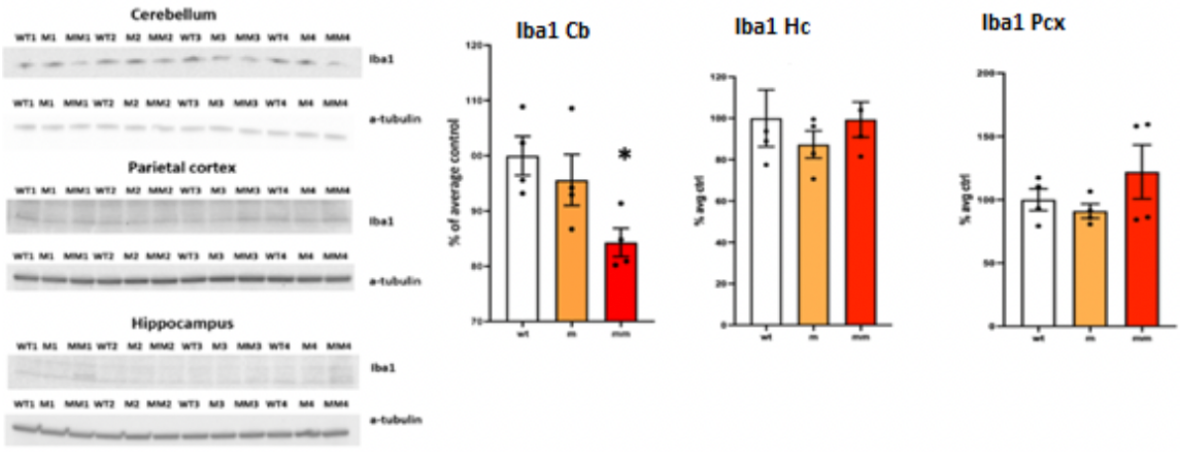

*Heterozygous mutation = m and homozygous mutation = mm

Figure 20 Iba1 is decreased on protein level in cerebellum of S111T/S111T animals. A) Immunoblot assessment of Iba1 protein lysates shows decreased Iba1 on the protein level only in cerebellum of S111T/S111T animals. Densitometric analysis of the immunoblots confirms significantly downregulated Iba1 compared to two the genotypes (A). *Sig ANOVA LSD post hoc test; error bars: SEM; $P < 0.05$: $n = 4$

Microglia are the resident immune cells in the CNS and play a key role in regulating brain development by inducing phagocytic activity during brain injury and inflammation. Any disturbance in the microglial activity has detrimental consequences. Immunoblot assessment of microglia – marked with Iba1 in respective genotypes showed a downregulated Iba1 (17 kDa) at the protein level only in cerebellum of S111T/S111T animals. Figure 20 C) immune blotting assessment also revealed several bands in hippocampus of S111T/S111T animals, suggested to be isoforms of Iba1, and were included in analysis of Iba1 in hippocampus. The mice displayed reduced microglia in cerebellum which may indicate reduced phagocytic activity.

3.4.2 *Iba1* (*Aif-1*) transcripts are increased in hippocampus and parietal cortex

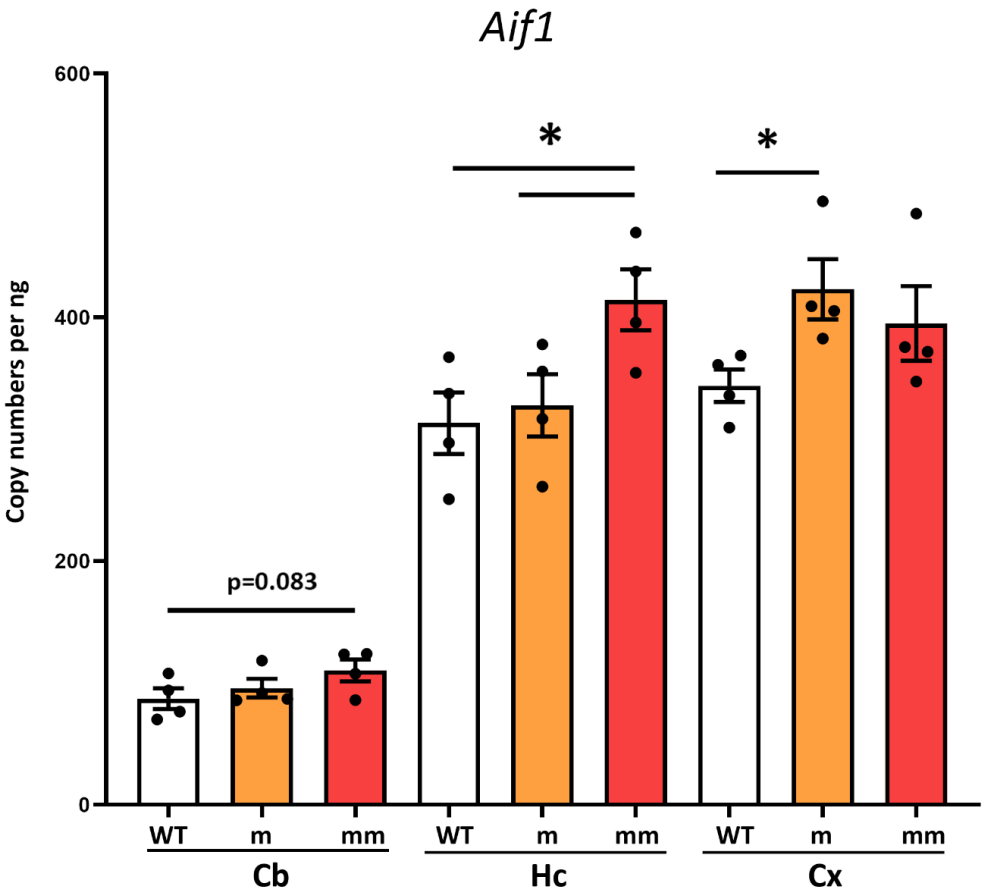

*Heterozygous mutation = m and homozygous mutation = mm

Figure 21 *Iba1 (Aif-1)* transcripts are increased in hippocampus and parietal cortex. RT-qPCR analysis of *Iba1* shows increased *Iba1* on mRNA level in S111T/S111T-animals in hippocampus compared to WT and WT/S111T. *Iba1* transcript were also significantly increased in WT/S111T (m) animals in parietal cortex compared to WT. *Sig ANOVA LSD post hoc test; error bars: SEM; $P < 0.05$; $n = 4$

Hypothetically, high expression of Iba1 – a marker of resident CNS immune cells is expected during neuroinflammation in pathological conditions. Investigation of *Iba-1 (Aif1*) shows upregulated *Iba1* transcripts in cerebellum of S111T/S111T animals compared with two genotypes. Additionally, upregulated *Iba1* was shown in hippocampus of WT/S111T animals compared with WT. The homozygous- and heterozygous mutation in AQP4 influences the mRNA expression of *Iba1*.

3.4.3 *Itgam* and *Cx3cr1* transcripts are upregulated in cerebellum of S111T/S111T animals

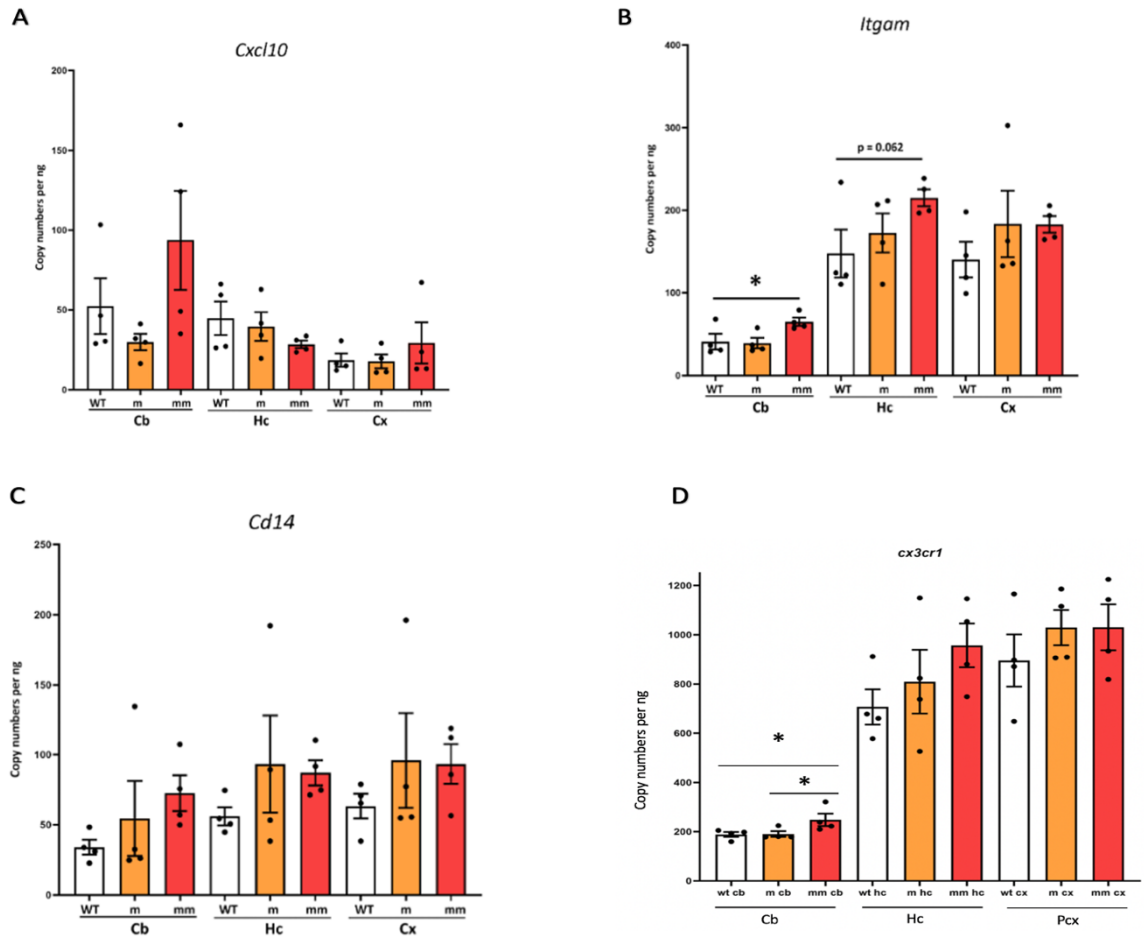

*Heterozygous mutation = m and homozygous mutation = mm

Figure 22 *Itgam* and *Cx3cr1* transcripts are upregulated in cerebellum of S111T/S111T animals. RT-qPCR analysis of microglial markers shows increased gene expression of *Itgam* and *Cx3cr1* in cerebellum only in S111T/S111T animals, compared to wild type. *Sig ANOVA LSD post hoc test; error bars: SEM; $P < 0.05$; $n = 4$

Figure 20 shows the protein levels of Iba1 were affected by S111T/S111T mutation in AQP4 in cerebellum, the transcript levels of microglia markers were further investigated by qPCR. It was reasonable to look at the transcript levels of the genes which are important for microglia activation, since their expression has previously shown remarkable downregulation during PD development and induced a pro-inflammatory response of AQP4. (Prydz et al., 2020).

We observed a significant upregulation of *Itgam* and *Cx3cr1* transcripts only in cerebellum. *Itgam* is a marker that code for microglia receptor named CD11b, and is involved in microglial

adhesion and migration (Prydz et al., 2020). *Cx3cr1* is fractalkine chemokine receptor, which is highly expressed in microglia. Deletion of *Cx3cr1* gene has previously been shown to induce a protective role during pathogenies (Wolf et al., 2013). Taken together with the observation that Iba1 is decreased on the protein level in cerebellum, the upregulation of *Itgam* and *Cx3cr1* in cerebellum indicates a differential regulation of microglia in S111T/S111T animals which may indicate an inflammation in progress.

3.5 Ser111Thr mutated AQP4: Cx43 expression and subcellular localization

As reported earlier, the AQP4-KO mouse model shows that connexin-43 is upregulated and compensate the loss of AQP4 by contributing to water transport in the brain (Katoozi et al., 2017). To see whether the astrocytic gap junctions are affected by the S111T mutation in AQP4 gen we performed an immunoblot analysis of this Cx43 in the three respective brain regions. Densitometric analysis revealed there was no significant changes in the expression on Cx43 at protein level between the genotypes (Appendix I).

4 Discussion

Despite more than 25 years after the first demonstration of AQP4 in the brain, there are still many questions regarding its pathophysiological function. Discovery of an AQP4 mutation in patient with pathological phenotype has given us an opportunity to investigate the causal role of AQP4 in the disease processes in the brain. For the first time, transgenic mice were generated using CRISPR/Cas9 technology to assess the effect of the S111T-AQP4 mutation shown to be pathogenic in a human patient.

Mutations affecting the function of AQP4 are crucial to provide knowledge about the role of AQP4 in the CNS. In this project, we chose to investigate the homozygous S111T/S11T mutated mouse model, as a homozygous mutation typically leads to a more severe phenotype. For immunofluorescence analysis, we only compared WT and homozygous mutated mice. When performing analysis on the molecular level, we included the heterozygous S111T mouse – which simulates the mutation identified in the patient.

It is notable that few significant changes were observed in the heterozygous mouse, which emulated the genotype of the patient. However, investigation of cerebellum, hippocampus, and parietal cortex revealed that majority of the findings are related to homozygous animals in cerebellum. Immunoblotting analysis showed downregulation of AQP4 and in addition higher molecular weight moiety of the water channel (Figure 14), while qPCR analysis revealed upregulated transcript levels of AQP4 (Figure 17). It is plausible that the mutation induces a change in the structural stability of AQP4 without affecting water permeability (Berland et al., 2018). Simultaneously, there was observed significant downregulation of the AQP4-ex isoform (Figure 16) which is necessary for the anchoring of AQP4 in perivascular end-feet. These findings support the fact that AQP4 stability might be affected due to low AQP4 turn-over in the plasma membrane only in cerebellum of S111T/S111T animals. Immunofluorescence of AQP4 along with protein of interest did not show any observable changes in the expression and subcellular localization. In addition, immunofluorescence does not have the sufficient resolution to assess subcellular regulation. Quantitative immunogold cytochemistry will be necessary to investigate whether subcellular localization of AQP4 is changed.

Interestingly, observation of downregulated microglia and upregulation of «risk gene» *Cx3cr1*, may suggest pro-inflammatory response of AQP4 in cerebellum. Taken together with the observation that both *Aqp4* and microglia markers were affected in the homozygous mutation

model, need to be discussed. One possibility for that might be due to high concentration of AQP4 in cerebellum which implies changes of the water channel in this region. Since no significant changes have so far been observed in the hippocampus and parietal cortex can be explained by the fact the disease is progressive, suggesting the condition worsens over time and changes in expression of AQP4 along with protein of interest may be age dependent.

4.1 Effects of S111T/S111T-AQP4 mutation in cerebellum

Upregulated APQ4 expression is a common denominator found in several neurological- and neurodegenerative diseases including MTLE, PD and AD (Eid et al., 2005; Prydz et al., 2020; Jing Yang et al., 2011). Investigation of S111T/S111T-AQP4 mutation revealed that AQP4 is downregulated on protein level in cerebellum (figure 14) while transcript levels are upregulated (figure 17). There was no correlation between protein- and transcript levels of *Aqp4*, suggesting that stability of AQP4 might be affected by the homozygous mutation in cerebellum. An immunolocalization of AQP4 was performed, no remarkable changes were observed between the two genotypes.

Berland et al 2018 suggest Ser111 is a phosphorylation site targeted by protein kinase A due to the amino acid sits in a motif that resembles the PKA phosphorylation site (Berland et al., 2018). The study also report that previous studies has shown that phosphorylation of Ser111-AQP4 in rat brain does not affect the function and expression of AQP4 (Assentoft et al., 2013; Berland et al., 2018; Kitchen et al., 2015) which in some extent contradicts with our findings. We observed no correlation between mRNA and protein levels of AQP4 (Figure 14 and 17) which possibly may indicate its expression is not regulated on gene levels but preferably on protein level. Theoretically, protein- and mRNA concentrations correlate to some extent, but such correlation is not always present. Post-transcriptional regulation is important for protein modification and its function, and approximately 40% of protein concentration is explained by mRNA abundances (Vogel & Marcotte, 2012). One possibility may be that higher turn-over may affect AQP4 synthesis which further affect the stability of AQP4 in the plasma membrane.

Notably, Silberstein et al 2004 shows that S111E-AQP4 mutation led to increased expression of M23-OAPs where they also concluded that Ser111 is phosphorylation site targeted by a PKA in regulation of AQP4 expression (Silberstein et al., 2004). This evidence contradicts the

findings in this project where S111T-AQP4 is downregulated and could possibly be explained by the difference in the mutated residues.

In the immunoblotting analysis, several higher bands of AQP4 (~200 kDa) were observed in cerebellum in S111T/S111T- animals (figure 14). Notably, so far, these higher bands have not been shown in any studies done while investigating S111-AQP4 mutations. Hypothetically, it might be that AQP4 is not downregulated but rather formed a complex with a higher molecular weight. The higher bands were only found in cerebellum (Figure 14) and not presented to that extent in the other regions which leads to an investigative question whether S111T/S111T-AQP4 mutation has an impact on the formation large clusters of AQP4.

The C-terminus of AQP4 is suggested to be important for AQP4 anchoring and astrocytic polarization due to its association with α-syntrophin and AQP4ex, which is important for AQP4 anchoring and localization. Additionally, M23-AQP4 is responsible to form the abundant OAPs in the plasma membrane while M1-AQP4 is not able to do that, due to extension of NH_2 group at the C-terminus that presumably prevent the OAPs formation (Nagelhus & Ottersen, 2013). Due to loss of AQP4 stability of S111T/S111T mice in cerebellum, we investigated the expression of AQP4ex only in that region. S111T/S111T animals displayed reduced AQP4-ex protein level in cerebellum (Figure 16). Regarding AQP4 anchoring, downregulated AQP4ex (Figure 16) could perhaps lead to less perivascular anchoring of S111T/S111T-AQP4, although we could not determine this by immunofluorescence microscopy.

4.2 Effects of S111T-AQP4 mutation on the expression of GFAP and Iba1

Microglia and astrocytes are two key cells in the brain and responsible for neuroinflammation. Neuroinflammation is an important hallmark observed in neurodegenerative diseases. Previous studies have shown an effect on the activation of microglia and its markers during pathological conditions including PD. Prydz et al 2020, is the first study to show that deletion of AQP4 results in less activation of microglia in a toxin-induced mouse model of PD, which further concluded that AQP4 plays a neuroinflammatory role during PD (Prydz et al., 2020). The pro-inflammatory role of AQP4 is explained by its involvement in the astrocyte-dependent activation of microglia. Also another study has suggested that AQP4 is important for the release of microglia-activating cytokines from astrocytes (Li et al., 2011).

To investigate if the pathogenic S111T-AQP4 mutation results a pro-inflammatory response, the expression of astrocytes and microglia markers (GFAP and Iba1 respectively) were investigated. Further investigation, immunofluorescence staining of GFAP of WT and S111T/S111T-animals did not reveal changes in the expression or localization, in the three respective brain regions. Immunoblotting analysis of GFAP in parietal cortex showed increased expression in S111T/S111T-AQP4 animals, compared to hippocampus and cerebellum.

Microglia are immune cells of the human brain and play an important role in maintaining neuronal homeostasis as they promote protective role during the development of neurodegenerative diseases including PD and AD. The presence of microglia during pathogenies is debatable due to their heterogenous expression which are termed as type M1 and M2. Presumably, these two types are shown to have opposite effect during neuroinflammation, where M1 are considered protective while M2 are involved in exacerbating detrimental conditions (Akhmetzyanova et al., 2019). Immunoblotting analysis of S111T/S111T-AQP4 animals showed downregulated microglia expression on protein level in cerebellum compared to WT (Figure 20). Usually, M1 type initiate phagocytic activity where they reduce aggregation and cellular toxicity in the brain. A downregulation of M1 can have major consequences and facilitate brain damage. It has been that depletion of microglia disrupt the neuronal development in olfactory bulb, indicating the importance of microglia for neural circuits (Wallace et al., 2020).

The inflammatory responses of microglia can be both beneficial and detrimental during pathogenesis depending on types of microglia are activated. So far there are no specific method available to distinguish the M1 and M2 types. However, investigation of microglial markers can indicate whether anti- or pro-inflammatory response is in progress. Important microglial genes revealed a global change in regulation of microglial activation in S111T/S111T-AQP4 animals which are only observed in cerebellum (Figure 22). Importantly, there was observed upregulation of *Cx3cr1* gene, which has both neuroprotective and neurotoxic role depending on the disease model (Lauro et al., 2015). Previous studies have showed that deficiency of CX3CR1 in microglia induce neuroprotective activity (Liu et al., 2010; Ridderstad Wollberg et al., 2014). During development of AD, absence of CX3CR1 increases the phagocytic activity of microglia nearby amyloid deposits which entails decreased amyloid levels (Liu et al., 2010). In addition, inhibition of chemokine receptors CX3CR1 reduces inflammation and degradation

of CNS in rat model for multiple sclerosis (MS) (Ridderstad Wollberg et al., 2014). In addition, S111T/S111T mice display upregulated *Itgam*, which is involved in microglial adhesion, in cerebellum. Other studies show that fly homolog of the human *ITGAM* receptor might be involved in modification of Tau proteins toxicity during development of AD (Shulman et al., 2014). Given this evidence, the upregulated *Cxc3r1* and *Itgam*, may indicate progression of neurotoxic activity in S111T/S111T-animals, and the mutation might entail pro-inflammatory response. Notably, there was not observed any significant changes in *Cd14* – key organizer of microglial inflammation (Janova et al., 2016). The downregulation of Iba1 on protein level in cerebellum (Figure 20) may display an immunosuppressive effect which is explained by the fact that phagocytic activity in the microglia is reduced in that brain region.

4.3 S111T-AQP4 might induce pro-inflammatory response in brain

The main findings of this project are regarding downregulated AQP4ex expression and increased expression of *Cx3cr1* cerebellum. CX3CR1 is a chemokine receptor involved in leukocyte adhesion and migration (Ridderstad Wollberg et al., 2014). In addition, upregulation of *Itgam* was observed in cerebellum. It encodes for Cd11b receptor, that is involved in microglial adhesion and migration (Prydz et al., 2020). Both genes are important for modulating microglial activity. It is possible that an inflammation in progress, since one can speculate that AQP4 is not well anchored due to a downregulation of AQP4-ex and microglia activity is changed, both at protein- and mRNA levels in cerebellum.

Our results shows that AQP4ex is more strongly affected by the S111T/S111T-AQP4 mutation (Figure 16) compared to the common AQP4 isoforms M1 and M23, which may have consequences for AQP4 anchoring. Previous studies have shown that AQP4ex deficient animals have resulted in smaller size of OAPs while the number is unaltered, simultaneous there was observed loss of astrocytic polarity in AQP4ex-KO animals (Palazzo et al., 2019). Concluding, the role of AQP4ex is important for AQP4 stability and polarization. In S111T/S111T-AQP4 animals, there was observed loss of AQP4 stability in cerebellum due to observation of no correlation between protein- and transcript levels of *Aqp4*, indicating an increased instability of AQP4 in the membrane (Figure 14 and 17). This actively indicates that Ser111 residue is involved in post-transcriptional regulatory mechanism in modification of AQP4. It is possible the Ser111 residue is involved in regulating AQP4ex expression where

downregulation of this isoform in cerebellum results in loss of AQP4 stability of S111T/S111T-animals. Evidence from in vitro studies of S111E mutated animals could support this, as it has been shown that the Ser111 residue is involved in AQP4 stability (Silberstein et al., 2004).

Immunolocalization of AQP4 (Figure 10) did not reveal any visible changes between the genotypes. Conducting quantitative immunogold analyzes where one can quantify the amount of AQP4 at the subcellular levels, and at the same time clarify the higher molecular weight found in the cerebellum of S111T/S111T-AQP4 animals will be an important for future works.

The changes observed in genes involved with microglia activity in the cerebellum suggest that non-channel functions of AQP4 is affected by S111T/S111T-AQP4 mutation. Changes in microglial genes have an inflammatory effect in the brain. (Prydz et al., 2020).

Pro-inflammatory response of AQP4 appears to be involved in exacerbating pathogenesis (Prydz et al., 2020). As previously reported, our findings suggest there might be an immunosuppressive response due to higher expression of *Cx3cr1* and displayed downregulated microglia protein level in cerebellum (Figure 20 and 22), suggesting reduced phagocytic activity in cerebellum. This findings is in line with previous study which showed that absence of *CX3CR1* during AD lead to higher phagocytic activity of microglia (Liu et al., 2010). Hypothetically, a chronic over-activation of CX3CR1 may lead to long-term brain damage.

Interestingly, a novel assessment of CX3CR1 in hippocampus shows the importance of the receptor during physiological conditions. Absence of CX3CR1 shows impairment cognitive function motor learning and associative memory in animals (Rogers et al., 2011). The involvement of CX3CR1 in physiological conditions raises an investigative question; whether phenotypes observed in the patient with S111T-AQP4 mutation are due to disturbances in the microglial activity. Although our findings are mainly related to cerebellum, but the involvement of CX3CR1 in physiological conditions suggests one possible hypothesis; that changes in microglial activity, due to upregulated *Cx3cr1* risk gene and downregulated microglia on protein level, may eventually result in changes in the physiology of the cerebellum including reduced motor control and cognition. The clinical presentation of the patient emphasizes that motor skills are most affected by the mutation which is strongly related to this brain region. Given that the role of AQP4 along with microglia and astrocytes in cerebellum is not well investigated, the S111T-AQP4 mutation may shed light on the important functions and roles of

this region for future work. It is difficult to speculate on anything yet. The disease is progressive which means the condition may worsen in other regions over time.

It is noteworthy to consider the significant increase in *Aqp4* on transcript levels in hippocampus compared to WT/S111T (Figure 17) and S111T/S111T mice displayed increased *Iba1 (Aif-1)* on transcript level in hippocampus compared to two genotypes (Figure 21). In addition, upregulation of GFAP on protein level is observed in parietal cortex only in S111T/S11T animals (Figure 18) along with upregulated *Iba1* on transcript level in WT/S111T compared to WT (Figure 21). Altogether, these findings suggest that expression of *Aqp4* and neuroinflammatory processes might also be altered in these regions, which might worsen over time.

Methodological considerations

For an overall assessment of the observable changes in *Aqp4* and microglial markers, it is important to acknowledge the methodological considerations. Mix gender animals were used in these experiments and due to the biological differences between the genders may affect the scientific output. In some cases, there was observed high variance in data which can be explained by the low numbers of animals (n = 4), from each genotype, were used to investigate the three respective regions.

4.4 Conclusion

The highly conserved serine residue in AQP4 has made researchers aware of its importance in terms of function and stability of the water channel. Mutations in S111 residue have previously shown no evidence to affect the stability and function of AQP4 in animal brain (Assentoft et al., 2013; Berland et al., 2018; Kitchen et al., 2015). Our assessment, of the first human pathogenic S111T-AQP4 mutation, shows that changes in AQP4 and AQP4-ex expression in cerebellum suggest that S111T-AQP4 mutation might influences stability and the non-channel functions of AQP4. AQP4-ex is most affected by mutation in Ser111 residue which indicates that downregulated AQP4-ex has a consequence for AQP4 stability and anchoring. Presumably, no correlation between transcript and protein levels of AQP4 (Figures 14 and 17) suggest that the Ser111 residue might be involved in post-transcriptional regulatory mechanism which determines the water channel stability.

Other study has suggested CX3CR1 might be involved in physiological conditions (Rogers et al., 2011), which lead to one possible unifying hypothesis that reduced motor control and cognition observed in the patient might be due to upregulation of microglial «risk gene»; *Cx3cr1* in cerebellum. S111T/S111T mice displayed reduced microglial expression on protein level in cerebellum (Figure 20), suggesting upregulation of the «risk gene» might decrease phagocytic activity and pro-inflammatory response may be in progress due to altered microglial activity in cerebellum. However, immunofluorescence showed fewer Iba1 positive microglia were observed in one of the S111T/S111T mice compared to the brain sections from other mice of both genotypes. More quantitative analysis must be conducted to assess whether the number of microglia is different in the two genotypes.

Overall, the findings correspond to phenotypes addressed in the patient with heterozygous Ser111Thr mutation, but in mice the severity of phenotypes seemed to be higher in animals with homozygous mutation compared to heterozygous mutation. It could also be possible that a heterozygous mutation in AQP4 leads to a more severe phenotype in the human brain, due to inter-species differences and different levels of CNS complexity.

4.5 Future studies

One could hypothesize that the wild-type allele in the heterozygous mouse compensate for the mutated AQP4 to some degree. The ratio of wild-type AQP4 and mutated AQP4 on the protein level should be investigated in future studies.

Since it seems like the anchoring of AQP4 is affected by S111T-AQP4 mutation further studies should include quantitative analysis by e.g., immunogold labeling where one can count the AQP4 expression in specific membrane domains. In addition, it would be interesting to look at other components involved in AQP4 anchoring such as dystrophin and α-syntrophin which may confirm if the astrocytic polarization if affected by this mutation.

The homozygous and heterozygous mice showed no overt phenotype, however behavioral and motor function tests were outside the scope of my project. The disease in the patient is progressive, and as we used 3–6-month-old adult mice in our study it will be important to study older mice, and to perform behavioral tests to shed light on whether the mutation model leads to motor and intellectual disability.

Due to downregulated microglia expression observed in cerebellum, a stereological cell count of microglia may reveal insights into the pro-inflammatory response of AQP4 in that brain region. For future work, it is necessary to have specific methods for differentiate heterogenous microglia and focus on research related to modifying microglial gene expression. The physiological role of microglial markers in cerebellum should be closely investigated to see if the functions of this region are affected by the changes in microglial genes expression. In addition, «risk genes», which are involved in development of neurodegenerative diseases, must be examined to confirm that microglial activity in cerebellum is detrimental. Considering all this, future studies may provide more insight into the effects of the pathogenic S111T-AQP4 mutation.

5 References

Abbott, N. J., Rönnbäck, L., & Hansson, E. (2006). Astrocyte–endothelial interactions at the blood–brain barrier. *Nature Reviews Neuroscience*, *7*(1), 41-53. https://doi.org/10.1038/nrn1824

Agre, P., King, L. S., Yasui, M., Guggino, W. B., Ottersen, O. P., Fujiyoshi, Y., Engel, A., & Nielsen, S. (2002). Aquaporin water channels--from atomic structure to clinical medicine. *J Physiol*, *542*(Pt 1), 3-16. https://doi.org/10.1113/jphysiol.2002.020818

Akhmetzyanova, E., Kletenkov, K., Mukhamedshina, Y., & Rizvanov, A. (2019). Different Approaches to Modulation of Microglia Phenotypes After Spinal Cord Injury [Review]. *Frontiers in Systems Neuroscience*, *13*(37). https://doi.org/10.3389/fnsys.2019.00037

Amann, B., Kleinwort, K. J. H., Hirmer, S., Sekundo, W., Kremmer, E., Hauck, S. M., & Deeg, C. A. (2016). Expression and Distribution Pattern of Aquaporin 4, 5 and 11 in Retinas of 15 Different Species. *International journal of molecular sciences*, *17*(7), 1145. https://doi.org/10.3390/ijms17071145

Amiry-Moghaddam, M., Frydenlund, D. S., & Ottersen, O. P. (2004). Anchoring of aquaporin-4 in brain: Molecular mechanisms and implications for the physiology and pathophysiology of water transport. *Neuroscience*, *129*(4), 997-1008. https://doi.org/https://doi.org/10.1016/j.neuroscience.2004.08.049

Amiry-Moghaddam, M., Otsuka, T., Hurn, P. D., Traystman, R. J., Haug, F.-M., Froehner, S. C., Adams, M. E., Neely, J. D., Agre, P., Ottersen, O. P., & Bhardwaj, A. (2003). An α-syntrophin-dependent pool of AQP4 in astroglial end-feet confers bidirectional water flow between blood and brain. *Proceedings of the National Academy of Sciences*, *100*(4), 2106-2111. https://doi.org/10.1073/pnas.0437946100

Amiry-Moghaddam, M., & Ottersen, O. P. (2003). The molecular basis of water transport in the brain. *Nature Reviews Neuroscience*, *4*(12), 991-1001. https://doi.org/10.1038/nrn1252

Amiry-Moghaddam, M., Williamson, A., Palomba, M., Eid, T., de Lanerolle, N. C., Nagelhus, E. A., Adams, M. E., Froehner, S. C., Agre, P., & Ottersen, O. P. (2003). Delayed K+ clearance associated with aquaporin-4 mislocalization: phenotypic defects in brains of alpha-syntrophin-null mice. *Proc Natl Acad Sci U S A*, *100*(23), 13615-13620. https://doi.org/10.1073/pnas.2336064100

Amiry-Moghaddam, M., Xue, R., Haug, F. M., Neely, J. D., Bhardwaj, A., Agre, P., Adams, M. E., Froehner, S. C., Mori, S., & Ottersen, O. P. (2004). Alpha syntrophin deletion removes the perivascular but not the endothelial pool of aquaporin-4 at the blood-brain barrier and delays the development of brain edema in an experimental model of acute hyponatremia. *FASEB J*, *18*(3), 542-544. https://doi.org/10.1096/fj.03-0869fje

Assentoft, M., Kaptan, S., Fenton, R. A., Hua, S. Z., de Groot, B. L., & MacAulay, N. (2013). Phosphorylation of rat aquaporin-4 at Ser111 is not required for channel gating. *Glia*, *61*(7), 1101-1112. https://doi.org/https://doi.org/10.1002/glia.22498

Attwell, D., Mishra, A., Hall, C. N., O'Farrell, F. M., & Dalkara, T. (2016). What is a pericyte? *Journal of cerebral blood flow and metabolism : official journal of the International Society of Cerebral Blood Flow and Metabolism*, *36*(2), 451-455. https://doi.org/10.1177/0271678X15610340

Au - Gage, G. J., Au - Kipke, D. R., & Au - Shain, W. (2012). Whole Animal Perfusion Fixation for Rodents. *JoVE*(65), e3564. https://doi.org/doi:10.3791/3564

Badaut, J., Fukuda, A. M., Jullienne, A., & Petry, K. G. (2014). Aquaporin and brain diseases. *Biochimica et Biophysica Acta (BBA) - General Subjects*, *1840*(5), 1554-1565. https://doi.org/https://doi.org/10.1016/j.bbagen.2013.10.032

Banerjee, S., & Bhat, M. A. (2007). Neuron-Glial Interactions in Blood-Brain Barrier Formation. *Annual Review of Neuroscience*, *30*(1), 235-258. https://doi.org/10.1146/annurev.neuro.30.051606.094345

Berland, S., Toft-Bertelsen, T. L., Aukrust, I., Byska, J., Vaudel, M., Bindoff, L. A., MacAulay, N., & Houge, G. (2018). A de novo Ser111Thr variant in aquaporin-4 in a patient with intellectual disability, transient signs of brain ischemia, transient cardiac hypertrophy, and progressive gait disturbance. *Cold Spring Harb Mol Case Stud*, *4*(1). https://doi.org/10.1101/mcs.a002303

Binder, D. K., Yao, X., Zador, Z., Sick, T. J., Verkman, A. S., & Manley, G. T. (2006). Increased seizure duration and slowed potassium kinetics in mice lacking aquaporin-4 water channels. *Glia*, *53*(6), 631-636. https://doi.org/https://doi.org/10.1002/glia.20318

Blandini, F., Nappi, G., Tassorelli, C., & Martignoni, E. (2000). Functional changes of the basal ganglia circuitry in Parkinson's disease. *Prog Neurobiol*, *62*(1), 63-88. https://doi.org/10.1016/s0301-0082(99)00067-2

Bojarskaite, L., Bjørnstad, D. M., Pettersen, K. H., Cunen, C., Hermansen, G. H., Åbjørsbråten, K. S., Chambers, A. R., Sprengel, R., Vervaeke, K., Tang, W., Enger, R., & Nagelhus, E. A. (2020). Astrocytic Ca2+ signaling is reduced during sleep and is involved in the regulation of slow wave sleep. *Nature Communications*, *11*(1), 3240. https://doi.org/10.1038/s41467-020-17062-2

Brodal, P. (2004). *The central nervous system: structure and function*. oxford university Press.

Brown, M. W., & Aggleton, J. P. (2001). Recognition memory: What are the roles of the perirhinal cortex and hippocampus? *Nat Rev Neurosci*, *2*(1), 51-61. https://doi.org/10.1038/35049064

Buchwalow, I. B., & Böcker, W. (2010). Immunohistochemistry. *Basics and Methods*, *1*, 1-149.

Burry, R. W. (2009). Immunocytochemistry. *Springer Science+ Business Media. DOI*, *10*, 978-971.

Chi, Y., Fan, Y., He, L., Liu, W., Wen, X., Zhou, S., Wang, X., Zhang, C., Kong, H., Sonoda, L., Tripathi, P., Li, C. J., Yu, M. S., Su, C., & Hu, G. (2011). Novel role of aquaporin-4 in CD4+ CD25+ T regulatory cell development and severity of Parkinson's disease. *Aging Cell*, *10*(3), 368-382. https://doi.org/https://doi.org/10.1111/j.1474-9726.2011.00677.x

Chung, W.-S., Clarke, L. E., Wang, G. X., Stafford, B. K., Sher, A., Chakraborty, C., Joung, J., Foo, L. C., Thompson, A., Chen, C., Smith, S. J., & Barres, B. A. (2013). Astrocytes mediate synapse elimination through MEGF10 and MERTK pathways. *Nature*, *504*(7480), 394-400. https://doi.org/10.1038/nature12776

Crane, J. M., Bennett, J. L., & Verkman, A. S. (2009). Live cell analysis of aquaporin-4 m1/m23 interactions and regulated orthogonal array assembly in glial cells. *The Journal of biological chemistry*, *284*(51), 35850-35860. https://doi.org/10.1074/jbc.M109.071670

Day, R. E., Kitchen, P., Owen, D. S., Bland, C., Marshall, L., Conner, A. C., Bill, R. M., & Conner, M. T. (2014). Human aquaporins: Regulators of transcellular water flow.

Biochimica et Biophysica Acta (BBA) - General Subjects, *1840*(5), 1492-1506. https://doi.org/https://doi.org/10.1016/j.bbagen.2013.09.033
Del Bigio, M. R. (2010). Ependymal cells: biology and pathology. *Acta Neuropathologica*, *119*(1), 55-73. https://doi.org/10.1007/s00401-009-0624-y
Domańska-Janik, K. (1996). Protein serine/threonine kinases (PKA, PKC and CaMKII) involved in ischemic brain pathology. *Acta Neurobiol Exp (Wars)*, *56*(2), 579-585.
Dudek, F. E., & Rogawski, M. A. (2005). Regulation of brain water: is there a role for aquaporins in epilepsy? *Epilepsy currents*, *5*(3), 104-106. https://doi.org/10.1111/j.1535-7511.2005.05310.x
Eid, T., Lee, T. S., Thomas, M. J., Amiry-Moghaddam, M., Bjørnsen, L. P., Spencer, D. D., Agre, P., Ottersen, O. P., & de Lanerolle, N. C. (2005). Loss of perivascular aquaporin 4 may underlie deficient water and K+ homeostasis in the human epileptogenic hippocampus. *Proc Natl Acad Sci U S A*, *102*(4), 1193-1198. https://doi.org/10.1073/pnas.0409308102
Fong, C. W. (2015). Permeability of the Blood–Brain Barrier: Molecular Mechanism of Transport of Drugs and Physiologically Important Compounds. *The Journal of Membrane Biology*, *248*(4), 651-669. https://doi.org/10.1007/s00232-015-9778-9
Freedman, D. J., & Ibos, G. (2018). An Integrative Framework for Sensory, Motor, and Cognitive Functions of the Posterior Parietal Cortex. *Neuron*, *97*(6), 1219-1234. https://doi.org/https://doi.org/10.1016/j.neuron.2018.01.044
Frydenlund, D. S., Bhardwaj, A., Otsuka, T., Mylonakou, M. N., Yasumura, T., Davidson, K. G. V., Zeynalov, E., Skare, Ø., Laake, P., Haug, F.-M., Rash, J. E., Agre, P., Ottersen, O. P., & Amiry-Moghaddam, M. (2006). Temporary loss of perivascular aquaporin-4 in neocortex after transient middle cerebral artery occlusion in mice. *Proceedings of the National Academy of Sciences*, *103*(36), 13532-13536. https://doi.org/10.1073/pnas.0605796103
Gunnarson, E., Zelenina, M., Axehult, G., Song, Y., Bondar, A., Krieger, P., Brismar, H., Zelenin, S., & Aperia, A. (2008). Identification of a molecular target for glutamate regulation of astrocyte water permeability. *Glia*, *56*(6), 587-596. https://doi.org/https://doi.org/10.1002/glia.20627
Haj-Yasein, N. N., Jensen, V., Østby, I., Omholt, S. W., Voipio, J., Kaila, K., Ottersen, O. P., Hvalby, Ø., & Nagelhus, E. A. (2012). Aquaporin-4 regulates extracellular space volume dynamics during high-frequency synaptic stimulation: A gene deletion study in mouse hippocampus. *Glia*, *60*(6), 867-874. https://doi.org/10.1002/glia.22319
Haseloff, R. F., Dithmer, S., Winkler, L., Wolburg, H., & Blasig, I. E. (2015). Transmembrane proteins of the tight junctions at the blood–brain barrier: Structural and functional aspects. *Semin Cell Dev Biol*, *38*, 16-25. https://doi.org/10.1016/j.semcdb.2014.11.004
Hiroaki, Y., Tani, K., Kamegawa, A., Gyobu, N., Nishikawa, K., Suzuki, H., Walz, T., Sasaki, S., Mitsuoka, K., Kimura, K., Mizoguchi, A., & Fujiyoshi, Y. (2006). Implications of the Aquaporin-4 Structure on Array Formation and Cell Adhesion. *J Mol Biol*, *355*(4), 628-639. https://doi.org/10.1016/j.jmb.2005.10.081
Hopperton, K. E., Mohammad, D., Trépanier, M. O., Giuliano, V., & Bazinet, R. P. (2018). Markers of microglia in post-mortem brain samples from patients with Alzheimer's disease: a systematic review. *Molecular Psychiatry*, *23*(2), 177-198. https://doi.org/10.1038/mp.2017.246
Jalali, M., Zaborowska, J., & Jalali, M. (2017). Chapter 1 - The Polymerase Chain Reaction: PCR, qPCR, and RT-PCR. In M. Jalali, F. Y. L. Saldanha, & M. Jalali (Eds.), *Basic*

Science Methods for Clinical Researchers (pp. 1-18). Academic Press. https://doi.org/https://doi.org/10.1016/B978-0-12-803077-6.00001-1

Janova, H., Böttcher, C., Holtman, I. R., Regen, T., van Rossum, D., Götz, A., Ernst, A.-S., Fritsche, C., Gertig, U., Saiepour, N., Gronke, K., Wrzos, C., Ribes, S., Rolfes, S., Weinstein, J., Ehrenreich, H., Pukrop, T., Kopatz, J., Stadelmann, C., Salinas-Riester, G., Weber, M. S., Prinz, M., Brück, W., Eggen, B. J. L., Boddeke, H. W. G. M., Priller, J., & Hanisch, U.-K. (2016). CD14 is a key organizer of microglial responses to CNS infection and injury. *Glia*, *64*(4), 635-649. https://doi.org/https://doi.org/10.1002/glia.22955

Jiang, F., & Doudna, J. A. (2017). CRISPR-Cas9 Structures and Mechanisms. *Annu Rev Biophys*, *46*(1), 505-529. https://doi.org/10.1146/annurev-biophys-062215-010822

Jung, J. S., Bhat, R. V., Preston, G. M., Guggino, W. B., Baraban, J. M., & Agre, P. (1994). Molecular characterization of an aquaporin cDNA from brain: candidate osmoreceptor and regulator of water balance. *Proceedings of the National Academy of Sciences*, *91*(26), 13052-13056. https://doi.org/10.1073/pnas.91.26.13052

Katoozi, S., Skauli, N., Rahmani, S., Camassa, L. M. A., Boldt, H. B., Ottersen, O. P., & Amiry-Moghaddam, M. (2017). Targeted deletion of Aqp4 promotes the formation of astrocytic gap junctions. *Brain Struct Funct*, *222*(9), 3959-3972. https://doi.org/10.1007/s00429-017-1448-5

Kim, S.-O., Kim, J., Okajima, T., & Cho, N.-J. (2017). Mechanical properties of paraformaldehyde-treated individual cells investigated by atomic force microscopy and scanning ion conductance microscopy. *Nano convergence*, *4*(1), 5-5. https://doi.org/10.1186/s40580-017-0099-9

Kim, Y., Park, J., & Choi, Y. K. (2019). The Role of Astrocytes in the Central Nervous System Focused on BK Channel and Heme Oxygenase Metabolites: A Review. *Antioxidants*, *8*(5), 121. https://www.mdpi.com/2076-3921/8/5/121

Kitchen, P., Day, R. E., Taylor, L. H. J., Salman, M. M., Bill, R. M., Conner, M. T., & Conner, A. C. (2015). Identification and Molecular Mechanisms of the Rapid Tonicity-induced Relocalization of the Aquaporin 4 Channel. *The Journal of biological chemistry*, *290*(27), 16873-16881. https://doi.org/10.1074/jbc.M115.646034

Koenig, M. A. (2018). Cerebral Edema and Elevated Intracranial Pressure. *Continuum (Minneap Minn)*, *24*(6), 1588-1602. https://doi.org/10.1212/CON.0000000000000665

Koziol, L. F., Budding, D., Andreasen, N., D'Arrigo, S., Bulgheroni, S., Imamizu, H., Ito, M., Manto, M., Marvel, C., Parker, K., Pezzulo, G., Ramnani, N., Riva, D., Schmahmann, J., Vandervert, L., & Yamazaki, T. (2014). Consensus Paper: The Cerebellum's Role in Movement and Cognition. *The Cerebellum*, *13*(1), 151-177. https://doi.org/10.1007/s12311-013-0511-x

Latal, B., Patel, P., Liamlahi, R., Knirsch, W., O'Gorman Tuura, R., von Rhein, M., on behalf of the Research Group, H., & Brain. (2016). Hippocampal volume reduction is associated with intellectual functions in adolescents with congenital heart disease. *Pediatric Research*, *80*(4), 531-537. https://doi.org/10.1038/pr.2016.122

Lauro, C., Catalano, M., Trettel, F., & Limatola, C. (2015). Fractalkine in the nervous system: neuroprotective or neurotoxic molecule? *Ann. N.Y. Acad. Sci*, *1351*(1), 141-148. https://doi.org/10.1111/nyas.12805

Li, J., & Verkman, A. S. (2001). Impaired hearing in mice lacking aquaporin-4 water channels. *The Journal of biological chemistry*, *276*(33), 31233-31237. https://doi.org/10.1074/jbc.M104368200

Li, L., Zhang, H., Varrin-Doyer, M., Zamvil, S. S., & Verkman, A. S. (2011). Proinflammatory role of aquaporin-4 in autoimmune neuroinflammation. *The FASEB Journal*, *25*(5), 1556-1566. https://doi.org/https://doi.org/10.1096/fj.10-177279

Liddelow, S. A., & Barres, B. A. (2017). Reactive Astrocytes: Production, Function, and Therapeutic Potential. *Immunity*, *46*(6), 957-967. https://doi.org/https://doi.org/10.1016/j.immuni.2017.06.006

Liddelow, S. A., Guttenplan, K. A., Clarke, L. E., Bennett, F. C., Bohlen, C. J., Schirmer, L., Bennett, M. L., Münch, A. E., Chung, W.-S., Peterson, T. C., Wilton, D. K., Frouin, A., Napier, B. A., Panicker, N., Kumar, M., Buckwalter, M. S., Rowitch, D. H., Dawson, V. L., Dawson, T. M., Stevens, B., & Barres, B. A. (2017). Neurotoxic reactive astrocytes are induced by activated microglia. *Nature*, *541*(7638), 481-487. https://doi.org/10.1038/nature21029

Liu, Z., Condello, C., Schain, A., Harb, R., & Grutzendler, J. (2010). CX3CR1 in microglia regulates brain amyloid deposition through selective protofibrillar amyloid-β phagocytosis. *J Neurosci*, *30*(50), 17091-17101. https://doi.org/10.1523/jneurosci.4403-10.2010

Lun, M. P., Monuki, E. S., & Lehtinen, M. K. (2015). Development and functions of the choroid plexus-cerebrospinal fluid system. *Nat Rev Neurosci*, *16*(8), 445-457. https://doi.org/10.1038/nrn3921

Ma, T., Yang, B., Gillespie, A., Carlson, E. J., Epstein, C. J., & Verkman, A. S. (1997). Generation and phenotype of a transgenic knockout mouse lacking the mercurial-insensitive water channel aquaporin-4. *The Journal of clinical investigation*, *100*(5), 957-962. https://doi.org/10.1172/JCI231

Mader, S., & Brimberg, L. (2019). Aquaporin-4 Water Channel in the Brain and Its Implication for Health and Disease. *Cells*, *8*(2). https://doi.org/10.3390/cells8020090

Mahmood, T., & Yang, P.-C. (2012). Western blot: Technique, theory, and trouble shooting [Technical Article]. *North American Journal of Medical Sciences*, *4*(9), 429-434. https://doi.org/10.4103/1947-2714.100998

Manley, G. T., Fujimura, M., Ma, T., Noshita, N., Filiz, F., Bollen, A. W., Chan, P., & Verkman, A. S. (2000). Aquaporin-4 deletion in mice reduces brain edema after acute water intoxication and ischemic stroke. *Nat Med*, *6*(2), 159-163. https://doi.org/10.1038/72256

Mathiisen, T. M., Lehre, K. P., Danbolt, N. C., & Ottersen, O. P. (2010). The perivascular astroglial sheath provides a complete covering of the brain microvessels: An electron microscopic 3D reconstruction. *Glia*, *58*(9), 1094-1103. https://doi.org/https://doi.org/10.1002/glia.20990

Mestre, H., Hablitz, L. M., Xavier, A. L., Feng, W., Zou, W., Pu, T., Monai, H., Murlidharan, G., Castellanos Rivera, R. M., Simon, M. J., Pike, M. M., Plá, V., Du, T., Kress, B. T., Wang, X., Plog, B. A., Thrane, A. S., Lundgaard, I., Abe, Y., Yasui, M., Thomas, J. H., Xiao, M., Hirase, H., Asokan, A., Iliff, J. J., & Nedergaard, M. (2018). Aquaporin-4-dependent glymphatic solute transport in the rodent brain. *eLife*, *7*, e40070. https://doi.org/10.7554/eLife.40070

Middeldorp, J., & Hol, E. M. (2011). GFAP in health and disease. *Progress in Neurobiology*, *93*(3), 421-443. https://doi.org/https://doi.org/10.1016/j.pneurobio.2011.01.005

Moe, S. E., Sorbo, J. G., Sogaard, R., Zeuthen, T., Petter Ottersen, O., & Holen, T. (2008). New isoforms of rat Aquaporin-4. *Genomics*, *91*(4), 367-377. https://doi.org/https://doi.org/10.1016/j.ygeno.2007.12.003

Nagelhus, E. A., & Ottersen, O. P. (2013). Physiological roles of aquaporin-4 in brain. *Physiol Rev*, *93*(4), 1543-1562. https://doi.org/10.1152/physrev.00011.2013

Nakahama, K.-I., Nagano, M., Fujioka, A., Shinoda, K., & Sasaki, H. (1999). Effect of TPA on aquaporin 4 mRNA expression in cultured rat astrocytes. *Glia*, *25*(3), 240-246.

https://doi.org/https://doi.org/10.1002/(SICI)1098-1136(19990201)25:3<240::AID-GLIA4>3.0.CO;2-C
Nayak, D., Roth, T. L., & McGavern, D. B. (2014). Microglia development and function. *Annual review of immunology*, *32*, 367-402. https://doi.org/10.1146/annurev-immunol-032713-120240
Nedergaard, M. (2013). Neuroscience. Garbage truck of the brain. *Science*, *340*(6140), 1529-1530. https://doi.org/10.1126/science.1240514
Neely, J. D., Amiry-Moghaddam, M., Ottersen, O. P., Froehner, S. C., Agre, P., & Adams, M. E. (2001). Syntrophin-dependent expression and localization of Aquaporin-4 water channel protein. *Proceedings of the National Academy of Sciences*, *98*(24), 14108-14113. https://doi.org/10.1073/pnas.241508198
Neely, J. D., Amiry-Moghaddam, M., Ottersen, O. P., Froehner, S. C., Agre, P., & Adams, M. E. (2001). Syntrophin-dependent expression and localization of Aquaporin-4 water channel protein. *Proc Natl Acad Sci U S A*, *98*(24), 14108-14113. https://doi.org/10.1073/pnas.241508198
Neely, J. D., Christensen, B. M., Nielsen, S., & Agre, P. (1999). Heterotetrameric Composition of Aquaporin-4 Water Channels. *Biochemistry*, *38*(34), 11156-11163. https://doi.org/10.1021/bi990941s
Nehring, S. M., Tadi, P., & Tenny, S. (2021). Cerebral Edema. In *StatPearls*. StatPearls Publishing

Nesverova, V., & Törnroth-Horsefield, S. (2019). Phosphorylation-Dependent Regulation of Mammalian Aquaporins. *Cells*, *8*(2), 82. https://www.mdpi.com/2073-4409/8/2/82
Nicchia, G. P., Cogotzi, L., Rossi, A., Basco, D., Brancaccio, A., Svelto, M., & Frigeri, A. (2008). Expression of multiple AQP4 pools in the plasma membrane and their association with the dystrophin complex. *Journal of Neurochemistry*, *105*(6), 2156-2165. https://doi.org/https://doi.org/10.1111/j.1471-4159.2008.05302.x
Nielsen, S., Nagelhus, E. A., Amiry-Moghaddam, M., Bourque, C., Agre, P., & Ottersen, O. P. (1997). Specialized membrane domains for water transport in glial cells: high-resolution immunogold cytochemistry of aquaporin-4 in rat brain. *J Neurosci*, *17*(1), 171-180. https://doi.org/10.1523/jneurosci.17-01-00171.1997
Pajarillo, E., Rizor, A., Lee, J., Aschner, M., & Lee, E. (2019). The role of astrocytic glutamate transporters GLT-1 and GLAST in neurological disorders: Potential targets for neurotherapeutics. *Neuropharmacology*, *161*, 107559-107559. https://doi.org/10.1016/j.neuropharm.2019.03.002
Palazzo, C., Buccoliero, C., Mola, M. G., Abbrescia, P., Nicchia, G. P., Trojano, M., & Frigeri, A. (2019). AQP4ex is crucial for the anchoring of AQP4 at the astrocyte end-feet and for neuromyelitis optica antibody binding. *Acta Neuropathologica Communications*, *7*(1), 51. https://doi.org/10.1186/s40478-019-0707-5
Parpura, V., & Verkhratsky, A. (2012). Astrocytes revisited: concise historic outlook on glutamate homeostasis and signaling. *Croatian medical journal*, *53*(6), 518-528. https://doi.org/10.3325/cmj.2012.53.518
Prydz, A., Stahl, K., Zahl, S., Skauli, N., Skare, Ø., Ottersen, O. P., & Amiry-Moghaddam, M. (2020). Pro-Inflammatory Role of AQP4 in Mice Subjected to Intrastriatal Injections of the Parkinsonogenic Toxin MPP+. *Cells*, *9*(11), 2418. https://www.mdpi.com/2073-4409/9/11/2418
Ridderstad Wollberg, A., Ericsson-Dahlstrand, A., Juréus, A., Ekerot, P., Simon, S., Nilsson, M., Wiklund, S.-J., Berg, A.-L., Ferm, M., Sunnemark, D., & Johansson, R. (2014). Pharmacological inhibition of the chemokine receptor CX3CR1 attenuates disease in a

chronic-relapsing rat model for multiple sclerosis. *Proceedings of the National Academy of Sciences of the United States of America*, *111*(14), 5409-5414. https://doi.org/10.1073/pnas.1316510111

Rogers, J. T., Morganti, J. M., Bachstetter, A. D., Hudson, C. E., Peters, M. M., Grimmig, B. A., Weeber, E. J., Bickford, P. C., & Gemma, C. (2011). CX3CR1 deficiency leads to impairment of hippocampal cognitive function and synaptic plasticity. *J Neurosci*, *31*(45), 16241-16250. https://doi.org/10.1523/jneurosci.3667-11.2011

Salter, M. W., & Stevens, B. (2017). Microglia emerge as central players in brain disease. *Nature Medicine*, *23*(9), 1018-1027. https://doi.org/10.1038/nm.4397

Shulman, J. M., Imboywa, S., Giagtzoglou, N., Powers, M. P., Hu, Y., Devenport, D., Chipendo, P., Chibnik, L. B., Diamond, A., Perrimon, N., Brown, N. H., De Jager, P. L., & Feany, M. B. (2014). Functional screening in Drosophila identifies Alzheimer's disease susceptibility genes and implicates Tau-mediated mechanisms. *Hum Mol Genet*, *23*(4), 870-877. https://doi.org/10.1093/hmg/ddt478

Silberstein, C., Bouley, R., Huang, Y., Fang, P., Pastor-Soler, N., Brown, D., & Hoek, A. N. V. (2004). Membrane organization and function of M1 and M23 isoforms of aquaporin-4 in epithelial cells. *American Journal of Physiology-Renal Physiology*, *287*(3), F501-F511. https://doi.org/10.1152/ajprenal.00439.2003

Silva, I., Silva, J., Ferreira, R., & Trigo, D. (2021). Glymphatic system, AQP4, and their implications in Alzheimer's disease. *Neurol Res Pract*, *3*(1), 5. https://doi.org/10.1186/s42466-021-00102-7

Smith, J. A., Das, A., Ray, S. K., & Banik, N. L. (2012). Role of pro-inflammatory cytokines released from microglia in neurodegenerative diseases. *Brain Res Bull*, *87*(1), 10-20. https://doi.org/10.1016/j.brainresbull.2011.10.004

Song, Y., & Gunnarson, E. (2012). Potassium Dependent Regulation of Astrocyte Water Permeability Is Mediated by cAMP Signaling. *PLOS ONE*, *7*(4), e34936. https://doi.org/10.1371/journal.pone.0034936

Sun, M.-K., & Alkon, D. L. (2012). Activation of Protein Kinase C Isozymes for the Treatment of Dementias. In E. K. Michaelis & M. L. Michaelis (Eds.), *Advances in Pharmacology* (Vol. 64, pp. 273-302). Academic Press. https://doi.org/https://doi.org/10.1016/B978-0-12-394816-8.00008-8

Tang, Y., & Le, W. (2016). Differential Roles of M1 and M2 Microglia in Neurodegenerative Diseases. *Mol Neurobiol*, *53*(2), 1181-1194. https://doi.org/10.1007/s12035-014-9070-5

Tani, K., Mitsuma, T., Hiroaki, Y., Kamegawa, A., Nishikawa, K., Tanimura, Y., & Fujiyoshi, Y. (2009). Mechanism of aquaporin-4's fast and highly selective water conduction and proton exclusion. *J Mol Biol*, *389*(4), 694-706. https://doi.org/10.1016/j.jmb.2009.04.049

Taylor, S., Wakem, M., Dijkman, G., Alsarraj, M., & Nguyen, M. (2010). A practical approach to RT-qPCR—Publishing data that conform to the MIQE guidelines. *Methods*, *50*(4), S1-S5. https://doi.org/https://doi.org/10.1016/j.ymeth.2010.01.005

Telano, L. N., & Baker, S. (2021). Physiology, Cerebral Spinal Fluid. In *StatPearls*. StatPearls Publishing

Underhill, S., & Amara, S. (2009). TRANSPORTERS | Glutamate Transporters in Epilepsy. In P. A. Schwartzkroin (Ed.), *Encyclopedia of Basic Epilepsy Research* (pp. 1398-

1405). Academic Press. https://doi.org/https://doi.org/10.1016/B978-012373961-2.00003-5
Vandebroek, A., & Yasui, M. (2020). Regulation of AQP4 in the Central Nervous System. *International journal of molecular sciences*, *21*(5), 1603. https://www.mdpi.com/1422-0067/21/5/1603
Verkhratsky, A., & Butt, A. (2007). *Glial neurobiology: a textbook*. John Wiley & Sons.
Verkman, A. S., Binder, D. K., Bloch, O., Auguste, K., & Papadopoulos, M. C. (2006). Three distinct roles of aquaporin-4 in brain function revealed by knockout mice. *Biochimica et Biophysica Acta (BBA) - Biomembranes*, *1758*(8), 1085-1093. https://doi.org/https://doi.org/10.1016/j.bbamem.2006.02.018
Vogel, C., & Marcotte, E. M. (2012). Insights into the regulation of protein abundance from proteomic and transcriptomic analyses. *Nat Rev Genet*, *13*(4), 227-232. https://doi.org/10.1038/nrg3185
Wallace, J., Lord, J., Dissing-Olesen, L., Stevens, B., & Murthy, V. N. (2020). Microglial depletion disrupts normal functional development of adult-born neurons in the olfactory bulb. *eLife*, *9*, e50531.
Wilhelmsson, U., Pozo-Rodrigalvarez, A., Kalm, M., de Pablo, Y., Widestrand, Å., Pekna, M., & Pekny, M. (2019). The role of GFAP and vimentin in learning and memory. *Biol Chem*, *400*(9), 1147-1156. https://doi.org/10.1515/hsz-2019-0199
Wolf, Y., Yona, S., Kim, K.-W., & Jung, S. (2013). Microglia, seen from the CX3CR1 angle. *Frontiers in cellular neuroscience*, *7*, 26-26. https://doi.org/10.3389/fncel.2013.00026
Woo, J., Kim, J. E., Im, J. J., Lee, J., Jeong, H. S., Park, S., Jung, S. Y., An, H., Yoon, S., Lim, S. M., Lee, S., Ma, J., Shin, E. Y., Han, Y. E., Kim, B., Lee, E. H., Feng, L., Chun, H., Yoon, B. E., Kang, I., Dager, S. R., Lyoo, I. K., & Lee, C. J. (2018). Astrocytic water channel aquaporin-4 modulates brain plasticity in both mice and humans: a potential gliogenetic mechanism underlying language-associated learning. *Molecular Psychiatry*, *23*(4), 1021-1030. https://doi.org/10.1038/mp.2017.113
Xu, Z., Xiao, N., Chen, Y., Huang, H., Marshall, C., Gao, J., Cai, Z., Wu, T., Hu, G., & Xiao, M. (2015). Deletion of aquaporin-4 in APP/PS1 mice exacerbates brain Aβ accumulation and memory deficits. *Molecular Neurodegeneration*, *10*(1), 58. https://doi.org/10.1186/s13024-015-0056-1
Xue, X., Zhang, W., Zhu, J., Chen, X., Zhou, S., Xu, Z., Hu, G., & Su, C. (2019). Aquaporin-4 deficiency reduces TGF-β1 in mouse midbrains and exacerbates pathology in experimental Parkinson's disease. *Journal of Cellular and Molecular Medicine*, *23*(4), 2568-2582. https://doi.org/https://doi.org/10.1111/jcmm.14147
Yamamoto, N., Sobue, K., Miyachi, T., Inagaki, M., Miura, Y., Katsuya, H., & Asai, K. (2001). Differential regulation of aquaporin expression in astrocytes by protein kinase C. *Brain Res Mol Brain Res*, *95*(1), 110-116. https://doi.org/10.1016/S0169-328X(01)00254-6
Yang, J., Lunde, L. K., Nuntagij, P., Oguchi, T., Camassa, L. M., Nilsson, L. N., Lannfelt, L., Xu, Y., Amiry-Moghaddam, M., Ottersen, O. P., & Torp, R. (2011). Loss of astrocyte polarization in the tg-ArcSwe mouse model of Alzheimer's disease. *J Alzheimers Dis*, *27*(4), 711-722. https://doi.org/10.3233/jad-2011-110725
Yang, J., Lunde, L. K., Nuntagij, P., Oguchi, T., Camassa, L. M. A., Nilsson, L. N. G., Lannfelt, L., Xu, Y., Amiry-Moghaddam, M., Ottersen, O. P., & Torp, R. (2011). Loss of Astrocyte Polarization in the Tg-ArcSwe Mouse Model of Alzheimer's Disease. *Journal of Alzheimer's Disease*, *27*, 711-722. https://doi.org/10.3233/JAD-2011-110725

Zhang, L., Zheng, Y., Xie, J., & Shi, L. (2020). Potassium channels and their emerging role in parkinson's disease. *Brain Research Bulletin*, *160*, 1-7. https://doi.org/https://doi.org/10.1016/j.brainresbull.2020.04.004

Zhou, B., Zuo, Y.-X., & Jiang, R.-T. (2019). Astrocyte morphology: Diversity, plasticity, and role in neurological diseases. *CNS Neuroscience & Therapeutics*, *25*(6), 665-673. https://doi.org/https://doi.org/10.1111/cns.13123

Zhou, X., Smith, Q. R., & Liu, X. (2021). Brain penetrating peptides and peptide–drug conjugates to overcome the blood–brain barrier and target CNS diseases. *WIREs Nanomedicine and Nanobiotechnology*, *13*(4), e1695. https://doi.org/https://doi.org/10.1002/wnan.1695

Zhou, Y., & Danbolt, N. C. (2014). Glutamate as a neurotransmitter in the healthy brain. *Journal of neural transmission (Vienna, Austria : 1996)*, *121*(8), 799-817. https://doi.org/10.1007/s00702-014-1180-8

6 Appendix I

6.1 Cx43 protein levels in cerebellum, hippocampus, parietal cortex is not significantly altered.

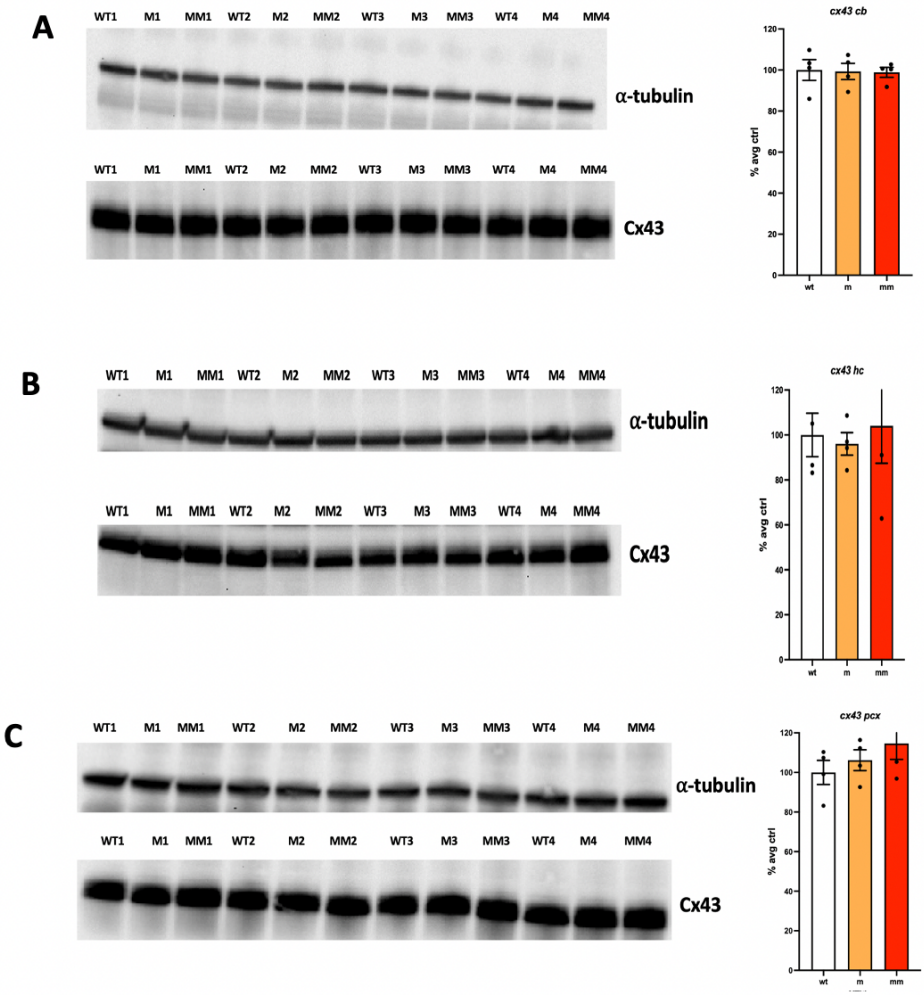

Figure 23 – Cx43 protein levels in cerebellum, hippocampus, parietal cortex is not significantly altered. Immunoblot assessment of Cx43 protein lysates shows no change in Cx43 expression on the protein level, in the three brain regions. *Sig ANOVA LSD post hoc test; error bars: SEM $P > 0.05$; n=4

7 Appendix II

Reagents and solutions

Immunofluorescence solutions

4% PFA

Solution I:

11.5 g Na_2HPO_4 in 800 mL dH_2O

40 g paraformaldehyde

Solution II:

2.3 g NaH_2HPO_4 in 200 mL dH_2O

1 L 0.01 M phosphate buffer saline (PBS)

8.76 g NaCl

0.20 g KCl

100 mL 0.1M phosphate buffer pH 7.4

900 mL dH_2O

Primary antibodies

- Rabbit anti-AQP4 antibidy Sigma-Aldrich
- Chicken anti-GFAP antibody Nordic Biosite AB
- Goat anti-Iba1 antibody Abcam

20 mL pre-incubation solution

2 mL Normal donkey serum (NDS)

0.2 g Bovine serum albumin (BSA)

2 mL Trition X-100

16 mL PBS

20 mL Primary antibody solution

2 mL NDS

0.2 g BSA

2 mL Trition X-100

16 mL PBS

20 mL Secondary antibody solution

600 µl NDS

0.2 g BSA

2 mL Triton X-100

17.4 mL

Secondary antibodies

- Cy2 anti-rabbit Jackson ImmunoResearch Laboratories
- Cy5 anti-chicken Jackson ImmunoResearchLaboratories
- Cy3 anti-goat Jackson ImmunoResearch Laboratorie

Solutions for western blot and RT-qPCR

RIPA buffer

0.8766 g NaCl

0.18612 g EDTA

0.5 g DOC

0.1 g SDS

Inhibitors:

cocktail PhosSTOP

protease inhibitor cocktail SigmaFAST

1x Laemmeli running Buffer

10x Laemmeli running buffer (30.3g Trizma base, Glycine, 10g SDS dissolved in 800ml dH_2O). To prepeare 1x Laemmeli running buffer: 100 ml of 10x Laemmeli running buffer dissolved in 900 ml dH_2O

1x Towbin transfer blotting buffer

10x Towbin blotting buffer (30.3 g Trizma base and 144.1 g Glycine, dissolve in 800 ml dH_2O). To prepare 1x Towbin transfer blotting buffer: 100 mL of 10x Towbin buffer dissolved in 200 mL ethanol/methanol and 700 mL H_2O

Master mix solutions for qPCR

2x Master mix: 10 µl

Forward Primer 10 µM: 0.4 µl

Reverse primer 10 µM: 0.4 µl

Template cDNA/Standards: 2 µl

H_2O: 7.2 µl

6x loading buffer

- 1.6 mL 1.5M Tris-HCl
- 0.42 g SDS
- 2.4 mL glycerol
- Trace amount of bromophenol blue
- 0.4 mL β-mercaptethanol
- 3.6 mL dH_2O